

**UCSF**

**UC San Francisco Electronic Theses and Dissertations**

**Title**

Using optogenetic tools to test the kinetic proofreading model of T cell receptor ligand discrimination

**Permalink**

<https://escholarship.org/uc/item/1m57x6rb>

**Author**

Tischer, Doug

**Publication Date**

2017

Peer reviewed|Thesis/dissertation

Using optogenetic tools to test the kinetic proofreading  
model of T cell receptor ligand discrimination  
by

Douglas Kyle Tischer

DISSERTATION

Submitted in partial satisfaction of the requirements for the degree of

DOCTOR OF PHILOSOPHY

in

Biochemistry and Molecular Biology

in the

GRADUATE DIVISION

of the

UNIVERSITY OF CALIFORNIA, SAN FRANCISCO

Copyright 2017

by

Doug Tischer

ii

For my parents,  
for their never ending love and support

## ACKNOWLEDGMENTS

I would first like to thank my advisor, Orion, for putting tremendous faith in me as a young grad student and allowing me to take on this very ambitious project. Besides a previous rotation, I had no experience researching cell signaling in the immune system. My project was a completely new direction for the lab as well. Prior to my project, the lab had no experience with T cell biology or questions about T cell receptor signaling. Additionally, the lab had no experience in much of the protein purifications methods that would be needed to troubleshoot these technically challenging projects. Despite it being extremely difficult and disheartening at times, Orion always only had support and encouragement. I don't know of many other PIs who would have taken a large leap of faith to allow a new graduate student to spearhead such a big change for the lab. I have grown incredibly from the experience.

To the other members of my thesis committee, Art Weiss, Jeroen Roose, Hana El-Samad, David Agard, thank you for having more confidence in me than I had in myself for much of the project. You always could always pry a path forward out of the most frustrating of data. I think it truly takes an optimist to be a PI.

I would like to give a special thanks to Art Weiss. Not only was he a member of my thesis committee, but he and his lab were invaluable scientific collaborators. I attended their weekly lab meetings, discussing the latest immunology papers with them and getting insightful feedback on my project. I used hardware in their lab when mine broke down, saving me from weeks of delays. I think I also managed to wring out over \$1500 in free Wednesday morning breakfasts over the years. To the many staff scientist and post-docs in Art's lab who were always so generous with their time, sharing reagents and protocols, thank you. Terri Kadlecsek, Byron Au-yeung, Haopeng Wang and Marianne Mollenauer. I honestly don't know how far I could have gotten without your support.

My other lab-away-from-lab was the Mullins lab. Peter Bieling, a post-doc at the time, single handedly taught me all I know about protein purification and completely turned my project around at a time when

it was struggling. Even after Peter left, the constant technical troubleshooting of the system required meant never ending rounds of protein purification. To this day I am amazed that no one batted an eye when I just dropped in start a prep. Instead they would greet me, eagerly ask how things were going and invite me to brewery tours with the lab. To everyone in the Mullins lab, thank you for always making me feel welcome and wanted.

My classmates made grad school memorable for more than just the science. Tuesday night volleyball games were always a highlight of my week and I'll never forget the Boston Market dinner we shared to celebrate our first win. At one time or another, these people made volleyball truly fun: Trevor Sorrells, John Leonard, Lindsey Pack (team captain!), Isabel Nocedal (thanks for organizing!), Kevin Mark, Coral Zhou, Tyler Faust, Kelly Nissen, Stefan Isaac, Liz Costa, Dustin Dovala (also a great Ping-pong partner), Alison Leaf, Scott Coyle (always ridiculously strong positive energy), Sam Liang and the occasional John Hansen (without whom we could never have a respectable spike). Go Squirrels!

To my best friends outside of school, thank you Duncan and Kim. Your love always reminded there is more to life than school. Without it, it's too easy to drown in the pressures and frustrations of research.

And of course to my parents, no amount of words can describe the support you have given me and how you prepared me for the world. When I do research, I can always see a bit of you reflected in it. My dad, by the way you are always a scientific sparring partner, to share my excitement with and to provide me perspective and guidance. My mom, by the way she always finds the creative solution to a problem. Though a needle and thread don't solve many problems in science, an eye for alternatives and workarounds is essential. All my love, Doug.

## STATEMENT REGARDING AUTHOR CONTRIBUTIONS

All approaches and experiments described in this dissertation were conceived of by Doug Tischer and Orion Weiner. All experiments were performed by Doug Tischer. All figures, graphs and tables were made by Doug Tischer.

Chapter Two is a reprint of a Perspective article Doug Tischer and Orion Weiner wrote for Nature Reviews Molecular Cell Biology and was published in August 2014 (volume 15, issue 8, pp 551–558). All figures and boxes in Chapter Two were originally produced by Doug Tischer and subsequently formatted by Nature Reviews Molecular Cell Biology to fit the journal's style.

# USING OPTOGENETIC TOOLS TO TEST THE KINETIC PROOFREADING MODEL OF T CELL RECEPTOR LIGAND DISCRIMINATION

Douglas Kyle Tischer

The kinetics and intensity of stimulation are thought to affect T cell signaling at multiple levels. For example, at the level of the receptor, ligand binding kinetics have been suggested to discriminate agonistic from non-agonist pMHCs. Downstream of the receptor, small changes in the intensity of stimulation can sharpen into a large all-or-nothing activation of Erk. However, precisely tuning the kinetics and intensity of stimulation and measuring the effects has remained challenging, limited in part by a lack of appropriate tools. Here we report the use of a LOV2-based optogenetic system to control the kinetics and intensity stimulation through a chimeric antigen receptor. Signaling through the receptor is initiated by the binding of LOV2 to the extracellular binding domain. Varying the intensity of blue light tunes the ligand binding kinetics from sub-second to tens of seconds. Other biophysical aspects of the interaction are not changed, allowing us to cleanly measure the effects ligand binding kinetics have on receptor signaling. Downstream of the receptor, titrating the intensity of blue light titrates the strength of the signal. By using several fluorescent live cell readouts of proximal signaling, we can measure single cell “dose response curves,” seeing if different portions of the signaling pathway respond in a linear, switch-like, adaptive or integrated manner to upstream signals. Optogenetic control of receptor signaling allows us to study T cell signaling with greater control than ever before, allowing us to directly ask how cells respond to changes in the kinetics and intensity of stimulation.



## TABLE OF CONTENTS

Chapter One: Introduction.....	1
Chapter Two: Illuminating cell signalling with optogenetic tools.....	12
Abstract.....	12
Introduction .....	12
Overview of optogenetic systems.....	13
Optogenetic control of cell signalling .....	16
Choosing an optogenetic system .....	18
Quantifying signal integration.....	22
Optogenetic control of signals in space .....	24
Optogenetic control of signals in time .....	26
Conclusions and perspectives .....	28
References .....	29
Chapter Three: Technical performance and troubleshooting of two optogenetic systems.....	47
PhyB purification and troubleshooting.....	47
PIF purification and troubleshooting .....	50
The LOVTRAP system .....	54
References .....	71
Chapter Four: Testing the kinetic proofreading model .....	72
Chapter Five: Protocols.....	85

Protocol 1: PhyB purification .....	85
Protocol 2: Alternative PhyB purification with a Pif affinity column .....	88
Light box for binding and eluting PhyB with light .....	88
Protocol 3: Pif conjugated protein purification .....	91
Protocol 4: LOV2 purification.....	93
Protocol 5: Zdk purification.....	96
Protocol 6: Buffer recipes for protein purification .....	97
Protocol 7: SUV formation .....	100
Protocol 8: RCA glass coverslip cleaning.....	104
Protocol 9: Kinetic proofreading experiments.....	105

## LIST OF TABLES

Box 1: Comparison of the reversible photosensitive proteins used in optogenetic systems .....	46
---	----

## LIST OF FIGURES

### Chapter Two

Figure 1: Different strategies for optogenetic inputs .....	37
Figure 2: Optogenetics for in vivo biochemistry .....	39
Figure 3: Optogenetic control of signals in space .....	42
Figure 4: Optogenetic control of signals in time.....	44

### Chapter Three

Figure 1: Comparing functionality of PhyB with and without four extra N-terminal amino acids.....	60
Figure 2: Pif3 has the largest dynamic range binding to PhyB of Pif1, Pif3 and Pif6 .....	62
Figure 3: A lower pH promotes SpyCatcher ligation.....	63
Figure 4: The majority of Pif molecules are active and capable of binding PhyB .....	64
Figure 5: PhyB retains significant activity after overnight incubation with cells.....	65
Figure 6: PhyB cannot induce signaling when Pif is conjugated to a cell-surface receptor .....	66
Figure 7: Titrating blue light intensity titrates the Zdk binding half-life .....	68
Figure 8: LOV2 recruitment to a Zdk-CAR is reversible and titratable.....	69
Figure 9: LOV2 remains active for hours.....	70

### Chapter Four

Figure 1: Example quantification of a light-stimulated time course.....	80
Figure 2: Zap70 recruits to the CAR without any proofreading steps .....	81

## CHAPTER ONE: INTRODUCTION

Your immune system is tasked with keeping you healthy by differentiating between self and non-self. It needs to recognize if a cell is part of the host or if another organism (virus, bacteria, amoeba, worms etc) is trying to replicate inside the body. Once an organism is recognized as foreign, the immune system moves to kill it and eliminate it from the body. This sweeping generalization of the immune system function is composed of many smaller functions, each of which is carried out by one of the numerous specialized cell types.

Conceptually, the immune system is broken into two parts: the innate and adaptive immune system. The evolutionarily older innate immune system recognizes pathogens with receptors that recognize fixed molecules produced by the pathogens. For example, cells in the innate immune system recognize formylated peptides produced by bacteria or double stranded RNA produced by some viruses. Once these fixed molecules are recognized, cells respond in a fixed manner. For example, cells can release noxious molecules to directly kill the pathogen, or help alert other cells to prepare for the infection. An important distinction is that cells of the innate immune system respond in the same way every time they encounter a pathogen. The response is stereotyped and does not change upon repeated exposure to a pathogen.

The unchanging response of the innate immune system contrasts with that of the adaptive immune system. The adaptive immune response is unique to each pathogen and responds more quickly to a secondary exposure. The two main cells of the adaptive immune system are T and B lymphocytes, so called because they mature in the thymus and bone marrow, respectively. The T and B cell receptors do not recognize predetermined molecules of invading pathogens. Instead, particular T and B cell clones that happen to recognize parts of a protein unique to the pathogen proliferate and respond in a unique way to that protein. B cells mature into plasma cells, which secrete antibodies that bind to the pathogen

protein that was recognized as foreign. Similarly, T cells can differentiate into cytotoxic T cell, which induce apoptosis in host cells that contain the pathogen protein.

Not only are the responses “adapted” to the particular pathogen, but so is the rate of response. Typically, the adaptive immune response peaks at 7-10 days after a primary infection. During the primary infection, a subset of T and B cells differentiate into long-lived memory cells. These memory cells active more easily and so respond faster upon a secondary infection of the same pathogen. The response of the adaptive immune system to a secondary infection is much faster and produces 100-1000 times more antibody. In that sense, the host has adapted to that particular pathogen, becoming more resistant to subsequent infections.

The adaptive immune system is very powerful. It allows us to adapt to surrounding pathogens and become resistant to their infection. As I write this thesis, it is also increasingly being used as a tool to fight cancer. Thus it is important to understand the fundamental biology and biophysics that activates the adaptive immune system in the first place. My thesis looks at the signaling mechanism of a central receptor in this activation process: the T cell receptor.

Activation of the adaptive immune system begins with the activation of CD4+ T helper cells. Subsequent proliferation and activation of B cells and CD8+ cytotoxic T cells are dependent on this initial activation. While each B cell clone has a unique specificity, they usually require the help of an activated CD4+ T helper cell to themselves activate. In effect, a CD4+ T cell “licenses” a B cell to start responding to its cognate antigen (the molecule the B cell receptor binds to). This licensing is beneficial in the context of an infection if the B cell antigen is on the pathogen. The subsequently generated antibodies will bind the pathogen, either neutralizing it directly and/or marking it for clearance. However, if a CD4+ T cell mistakenly recognizes a molecule from the host, it can license B cells to produce antibodies against host molecules. This is one driver of autoimmune disorders. A T cell’s specificity and ability to discriminate ligands is central

to the adaptive immune system's ability to appropriately respond to pathogens while avoiding damaging autoimmune responses.

T cells activate when they encounter antigen presenting cells (APCs) in lymph nodes. The APCs display small peptide fragments (about 13-17 amino acids<sup>1</sup>) on the cell surface bound to the major histocompatibility complex (MHC) class II. APCs continually display peptides derived from proteins in the cell and the surrounding environment. The vast majority will be "self-peptides," peptides derived from host proteins. During an infection, APCs will occasionally take up and display foreign peptides, derived from proteins of the pathogen. In effect, APCs continually display a sample of the current proteome of the host. Any peptides that are displayed that are not encoded in the host genome are a red flag of infection.

APCs themselves do not recognize a displayed peptide as self or foreign; CD4+ T cells do. CD4+ T cells continually scan the surface of APCs in lymph nodes, looking for foreign peptides. On a molecular level, a T cell recognizes the peptide-major histocompatibility complex (pMHC) through its T cell receptor (TCR). The T cell receptor is a complex of eight proteins: one CD3 $\epsilon$ -CD3 $\gamma$  heterodimer, one CD3 $\epsilon$ -CD3 $\delta$  heterodimer, one CD3 $\zeta$  homodimer and one heterodimer of the TCR  $\alpha$  and  $\beta$  chains<sup>2</sup>. The alpha and beta chains are each made up of two immunoglobulin domains, and bind one another like the heavy and light chains of the Fab fragment of an antibody. The end of the TCR alpha/beta complex binds the pMHC head on, with the MHC's central groove holding the peptide down its length. Thus the end of the TCR alpha/beta complex binds parts of both the MHC and the peptide. The nature of this interaction ultimately determines if a T cell activates in response to a peptide. Exactly what about the interaction activates signaling from some peptides but not others is a central and fundamental question in immunology.

A fundamental difference between how the T cell receptor bind its ligand from how most other receptor bind their ligand is that amount of diversity at the interface. Most receptors are entirely germ-line

encoded and bind an invariant ligand. Receptor and ligand have coevolved with each other, enabling evolution to select an interaction with high specificity and low cross-reactivity. By contrast, every surface at the TCR-pMHC binding interface is either not directly germline encoded or highly polymorphic. The loops at the end of the TCR alpha/beta subunits that bind pMHC are created through V(D)J recombination, a process of somatic DNA rearrangement, and further diversified by P- and N-nucleotide insertion. While the MHC itself is germline encoded, there are thousands of human polymorphisms, with most of the affected amino acids occurring at or near the binding interface. Finally, the peptides themselves are a near endless source of diversity. While all self-peptides are obviously germ line encoded, all the foreign peptide that the T cell needs to recognize are not. As MHCs promiscuously bind peptides, the diversity of presented foreign peptides is incredibly large.

The near limitless diversity at the TCR-pMHC binding interface poses a problem: how can each T cell receptor use a common mechanism to recognize its cognate pMHC when the binding interface is so diverse? A very common way that other receptors recognize their ligand is to use ligand-induced allosteric changes to initiate downstream signaling. These allosteric changes often rely on specific residue-residue contacts. Therefore it is hard to imagine how the diverse TCR-pMHC binding interface could reliably induce the same conformational change in the T cell receptor to initiate signaling.

Initial experiments showed that there was a poor correlation between the affinity of pMHC-TCR binding and the amount of signaling the pMHC induced<sup>3</sup>, suggesting that a more complex model must explain ligand discrimination by the TCR. In the mid 1990's, McKeithan put forward the kinetic proofreading model of ligand discrimination<sup>4</sup>, built off of the kinetic proofreading models for the enhanced fidelity of translation<sup>5</sup>. The model states that it is the dwell time of the TCR-pMHC interaction, rather than the strength of the interaction, that determines how stimulatory a pMHC is. At its core, what this means is that there is a delay between ligand binding and receptor signaling. This waiting period is made up of a number of irreversible signaling steps that require persistent ligand binding to complete. If the ligand



dissociates, the system immediately resets to the initial state. With this model, it is easy to see how ligands with a longer dwell time are more likely to induce signaling. Indeed, experiments seemed to suggest a better correlation between ligand potency and dwell time, rather than binding affinity<sup>5,6</sup>.

There are several experimental shortcomings that make the kinetic proofreading model far from settled. The first is the technique for measuring TCR-pMHC affinity. Until recently, the TCR-pMHC interaction was measured by surface plasmon resonance (SPR) in which one component is immobilized to a chip while the other is flowed in and then chased out<sup>3</sup>. This technique measures a “3D” affinity, meaning the two protein complexes are free to move in all directions when they bind and dissociate. But in vivo, the TCR and pMHC are confined to bind each other from two opposing membranes and there is no guarantee that 3D affinities are reflective of binding affinities in the 2D environment. While recent techniques for measuring such a 2D affinity have shown that more stimulatory pMHCs have longer dwell times, they also have higher on-rate constants. The on-rate constants span several more orders of magnitude than do the off rates<sup>7</sup>, suggesting that it might be easier for a receptor to discriminate pMHCs based on their on-rate rather than their off-rate. Sadly however, there is no model for how a cell might measure the on-rate of a ligand in the way that kinetic proofreading explains how a cell measures the ligand off rate.

A second shortcoming of current technique is that point mutation in the peptide are used to alter its binding kinetics to the TCR. Absent the optogenetic techniques presented here, there is no way to alter ligand binding kinetics without altering the binding surface in some way. This is not to fault using point mutants to study TCR ligand discrimination, only to point out some of their shortcomings and how they might be addressed. There are many ways to biophysically characterize the binding between a receptor and its ligand: the on-rate, the off-rate, binding affinity, orientation of binding, performance under load, the distance between opposing membranes and so on. Introducing a point mutation and observing a change in the off-rate does not mean that is the only change to the interaction. Other aspects of the interaction, either not measured or unknown, may also change and be responsible for a change in ligand

potency. In short, experiments that introduce point mutations to the peptide are observational. They do not directly alter ligand dwell time and so cannot definitively show that longer ligand dwell times cause more receptor signaling.

Because the kinetic proofreading model is the dominant model explaining ligand discrimination by the T cell receptor and its importance in directing the adaptive immune response, I set out to rigorously test the kinetic proofreading model by directly manipulating ligand binding kinetics with optogenetic inputs and observing how the receptor signals. Do differences in ligand binding half-lives fully account for differences in ligand agonism or might other aspects of the interaction also affect agonism? Does changing the ligand dwell time affect receptor signaling at all? The field needs direct experimental evidence to answer these questions and to directly support or refute the kinetic proofreading model.

To directly test the kinetic proofreading model, one needs to directly manipulate the dwell time of the receptor-ligand interaction. Here, optogenetics provides some fantastic tools. (Broadly speaking, optogenetics is the use of light sensitive proteins to manipulate cell signaling or function. For an in depth review of the field, see the section on my optogenetics review for Nature Reviews Molecular Cell Biology.)

Many optogenetic systems involve the light regulated interaction between two proteins: one is a light sensitive that changes conformation upon exposure to certain wavelengths of light and the other is a binding partner that selectively binds one of these conformations. As these proteins respond to light, they can induce protein-protein binding or unbinding on the order of seconds. This ability to dictate when and where two proteins interact is a perfect tool to test if the length of a ligand-receptor interaction (really, just another protein-protein interaction) affects signaling. Thus to test the kinetic proofreading model, I sought to substitute a light-gated protein-protein interaction for the native ligand-receptor interaction.

The strategy for replacing the native ligand-receptor interaction with a light-gated interaction took advantage of some peculiarities of the TCR. Only ligands bound to a solid surface are able to stimulate

the TCR. Monomeric ligands in solution do not induce signaling<sup>8</sup>. (There are two models to explain this fact: 1) The TCR could be mechanosensitive<sup>9,10</sup>. 2) A closely opposed surface is needed to exclude the bulky extracellular domain of the transmembrane phosphatase CD45<sup>1</sup>, which dephosphorylates the receptor, hindering its signaling. These models are not mutually exclusive.) These facts hold even for non-pMHC ligands. Fab fragments from otherwise stimulatory antibodies poorly stimulate the TCR<sup>1</sup>.

The strategy for light-gated control of ligand dwell time is to present a purified light-sensitive protein on a supported lipid bilayer and expose them to T cells expressing a TCR tagged with the corresponding interaction partner. Light could then either initiate or terminate the interaction between the receptor and light-sensitive protein on the supported lipid bilayer. Engineering this light-gated receptor-ligand interaction took years of work. The details of the engineering effort are laid out in the “Troubleshooting” section, but I will summarize it briefly here.

Initially, I used the PhyB/Pif system as it allowed both binding and unbinding to be controlled by light. Although the two purified proteins interacted robustly in vitro, Pif lost its ability to bind PhyB once it was on the surface of a cell. All genetic fusion of Pif to the N-terminus of a chimeric antigen receptor (a single transmembrane protein that mimics the TCR by having an extracellular interaction domain and intracellular ITAMs from CD3z) or the native TCR failed to reach the surface. Post-translationally ligating Pif to either the TCR or CAR resulted in complete loss of activity. After extensive troubleshooting, the reason(s) for the loss of activity are unknown. I suspect that Pif denatures when on the cell surface, due to the near total absence of any predicted secondary structure.

After giving up on the PhyB/Pif system, I switched to the LOVTRAP system<sup>11</sup> which consists of the wt LOV2 domain from *Avena sativa* and an engineering binding partner, Zdk. This system stood out amongst the many other optogenetic systems because it is one of the few where light stimulates the dissociation of pair, rather than their association. LOV2 purified without issue and luckily, a genetic fusion of Zdk to a CAR

trafficked to the surface and photo-reversibly bound LOV2. What's more, Jurkat cells expressing the CAR photo-reversibly signaled when dropped onto an SLB functionalized with LOV2. The full details of the experiment and the results are presented in the Results section.

Lastly, it is worth pointing out that my use of the LOVTRAP system can answer more biological questions than testing the kinetic proofreading model. The LOV2 systems gives full temporal and spatial control of T cell signaling at the highest level, a powerful tool to understand how the signaling cascade as a whole functions. By ramping stimulation up and then down, one can check for and quantify pathway hysteresis, a property useful in cellular decision making. Because you can monitor ligand binding in real time, one can quantify the amount of stimulation an individual cell experiences and even adjust it over time in response cell movement or signaling. Because the system is titratable, one can generate dose-response curves, rigorously characterizing the protein-based signaling circuit as an engineer might characterize an electronic circuit.

This tools need not be limited to the TCR. Many other cell surface immune receptors modify the primary signaling through the TCR pathway and are amenable to this type of optogenetic control. Given the robust performance with a CAR, I suspect it would take little more work than fusion Zdk to receptor's extracellular domain.

It would be interesting to present LOV2 on the surface of an APC, rather than a bilayer, to manipulate T cell signaling in a more cellular context with the added subtleties of the other cell surface receptors, rather than a minimalistic SLB system. Likely, LOV2 would have to be post-translationally ligated (e.g. by the SpyCatcher system<sup>12</sup>), as it does not tolerate fusions to its C-terminus (it sterically blocks Zdk binding). Alternatively, another LOV2 optogenetic system like iLID<sup>13</sup> could be used, as LOV2 is more tolerant of fusions to its C-terminus with this system. If both LOV2 and Zdk could be expressed genetically on the cell surface of APCs and T cell (respectively), it would be an exciting but ambitious project to use the system

in living mice to precisely control when and where T cells are activated. Paired with intravital imaging, it would be a powerful tool to understand T cell signaling in a totally *in vivo* context.

Before diving into the technical matters concerning the purification and activity of the optogenetic systems used here, it is useful to consider why these systems were chosen in the first place and how they compare to other available optogenetic systems. The following perspective paper Orion and I wrote serves as a good overview of available optogenetic systems, their similarities and difference, and how to choose the one best suited for a particular experiment. It appeared in Nature Reviews Molecular Cell Biology in August 2014.

## References

1. Davis, S. J. & van der Merwe, P. A. The kinetic-segregation model: TCR triggering and beyond. *Nat. Immunol.* **7**, 803–809 (2006).
2. de la Hera, a, Müller, U., Olsson, C., Isaaz, S. & Tunnacliffe, a. Structure of the T cell antigen receptor (TCR): two CD3 epsilon subunits in a functional TCR/CD3 complex. *J. Exp. Med.* **173**, 7–17 (1991).
3. Matsui, K., Boniface, J. J., Steffner, P., Reay, P. a & Davis, M. M. Kinetics of T-cell receptor binding to peptide/I-Ek complexes: correlation of the dissociation rate with T-cell responsiveness. *Proc. Natl. Acad. Sci. U. S. A.* **91**, 12862–6 (1994).
4. McKeithan, T. W. Kinetic proofreading in T-cell receptor signal transduction. *Proc. Natl. Acad. Sci. U. S. A.* **92**, 5042–6 (1995).
5. Hopfield, J. Kinetic proofreading: a new mechanism for reducing errors in biosynthetic processes requiring high specificity. *Proc. Natl. Acad.* **71**, 4135–4139 (1974).
6. Daniels, M. a *et al.* Thymic selection threshold defined by compartmentalization of Ras/MAPK signalling. *Nature* **444**, 724–9 (2006).
7. Huang, J. *et al.* The kinetics of two-dimensional TCR and pMHC interactions determine T-cell responsiveness. *Nature* **464**, 932–6 (2010).
8. Xie, J. *et al.* Photocrosslinkable pMHC monomers stain T cells specifically and cause ligand-bound TCRs to be 'preferentially' transported to the cSMAC. *Nat. Immunol.* **13**, 674–681 (2012).
9. Kim, S., Takeuchi, K., Sun, Z. & Touma, M. The  $\alpha\beta$  T cell receptor is an anisotropic mechanosensor. *J. Biol.* (2009).

10. Hu, K. H. & Butte, M. J. T cell activation requires force generation. *J. Cell Biol.* **213**, 535–542 (2016).
11. Wang, H. *et al.* LoVtraP: an optogenetic system for photoinduced protein dissociation. doi:10.1038/Nmeth.3926
12. Zakeri, B. *et al.* PNAS Plus: Peptide tag forming a rapid covalent bond to a protein, through engineering a bacterial adhesin. *Proceedings of the National Academy of Sciences* **109**, E690–E697 (2012).
13. Guntas, G. *et al.* Engineering an improved light-induced dimer (iLID) for controlling the localization and activity of signaling proteins. *Proc. Natl. Acad. Sci. U. S. A.* **112**, 112–7 (2015).

## CHAPTER TWO: ILLUMINATING CELL SIGNALLING WITH OPTOGENETIC TOOLS

Doug Tischer and Orion Weiner

Nat Rev Mol Cell Biol. 2014 Aug; 15(8): 551–558.

### Abstract

The light-based control of ion channels has been transformative for the neurosciences, but the optogenetic toolkit does not stop there. An expanding number of proteins and cellular functions have been shown to be controlled by light, and the practical considerations in deciding between reversible optogenetic systems (such as systems that use light-oxygen-voltage domains, phytochrome proteins, cryptochrome proteins and the fluorescent protein Dronpa) are well defined. The field is moving beyond proof of concept to answering real biological questions, such as how cell signalling is regulated in space and time, that were difficult or impossible to address with previous tools.

### Introduction

With the proper reagents, light can be used to observe and perturb the spatiotemporal dynamics of signals in living cells and organisms. The first attempts to acutely control cell signalling with light chemically ‘caged’ small molecule messengers by covalently attaching photolabile chemical groups at positions that are necessary for signalling. Upon exposure to light, these groups would cleave and dissociate, thereby ‘uncaging’ the molecule to signal in the cell. However, the engineering challenges in making these tools suitable for diverse signalling pathways and the difficulty in delivering them to cells and organisms limited their use<sup>1,2</sup>. Then optogenetics came along — the genetic encoding of light-sensitive proteins that activate signalling pathways in response to light. Its first application was the use of light-gated ion channels to



manipulate the excitability of neuronal cells<sup>3-5</sup>. With optogenetics, it no longer takes a chemist to produce the light-sensitive reagents, uncaging is no longer irreversible and the light-controlled proteins are much easier to deliver (and thus a greater level of spatial control is possible), because they can be expressed rather than injected. Investigators have taken advantage of the spatial precision of proteins that either hyperpolarize or depolarize neurons<sup>3-6</sup> to non-invasively identify the pacemaker cells in the zebrafish heart<sup>7</sup>, and used the temporal precision and reversibility of these proteins to elucidate the importance of timing in neuronal activity for behavioural conditioning<sup>8</sup>.

A limitation of these neuronal optogenetic tools is that they can only control membrane potential, and there are a wide range of other cellular and developmental biology questions that require the manipulation of other processes that affect cell signalling, such as protein localization, post-translational modification, GTP loading, and so on. With the adoption of other genetically encoded light-responsive proteins, the optogenetic toolkit has markedly expanded to include a wide array of regulatory proteins, and consequently cellular functions, which can now be controlled with light. Here, we first review the various optogenetic systems and practical considerations in using them. Then, we address the types of cell signalling questions that are being investigated with these approaches. Finally, we discuss future opportunities for the development of optogenetic tools.

## Overview of optogenetic systems

Proteins that change conformation in response to light have been adapted to regulate a wide array of signalling activities in living cells. Here, we discuss the optogenetic systems that are reversible and can be adopted to control a variety of signalling pathways. Three are based on photosensitive plant proteins (cryptochromes<sup>9-11</sup>, light-oxygen-voltage (LOV) domains<sup>12-15</sup> and phytochromes<sup>16-18</sup>), and one is based on

the fluorescent protein Dronpa<sup>19</sup>, which was isolated from the coral Pectiniidae<sup>20</sup>. Other recent publications discuss the use of optogenetic proteins that manipulate specific signalling events, such as those that regulate neuronal excitability<sup>4,21</sup>, cyclic nucleotides<sup>22,23</sup> and heterotrimeric G protein signalling<sup>24,25</sup>, or proteins that are irreversibly activated<sup>26–28</sup> or inactivated<sup>29</sup> by light.

#### *The PHYTOCHROME B protein*

PHYTOCHROME B (PHYB) is a protein that is activated by red light (650 nm) and inactivated by infrared light (750 nm), and normally controls seedling stem elongation in *Arabidopsis thaliana*. When expressed in cells, the apo-PHYB protein (which is chromophore free) only becomes light sensitive when it autocatalytically ligates to PCB, a chromophore that is present in photosynthetic organisms; however, in non-photosynthetic organisms, PCB must be delivered to cells directly or through the expression of the bio-synthetic enzymes that produce it<sup>30,31</sup>. Upon exposure to red light, PHYB that is bound to PCB changes conformation and binds to a PHYTOCHROME INTERACTING FACTOR (Pif) protein<sup>16</sup> within seconds. This association is reversed within seconds upon exposure to infrared light or is stable for hours in the dark<sup>18</sup>.

#### *The CRYPTOCHROME 2 protein*

CRYPTOCHROME 2 (CRY2) is a protein from *A. thaliana* that is sensitive to blue light (405–488 nm). Two changes occur upon exposure to blue light: the light-sensitive CRY2 protein homo-oligomerizes<sup>11</sup> and binds to its binding partner, CIB1 (CRYPTOCHROME-INTERACTING BASIC HELIX–LOOP–HELIX 1)<sup>32</sup>, both within seconds<sup>10</sup>. In the dark, CRY2 previously activated with blue light resets to its initial state within ~5 minutes. CRY2 uses the ubiquitously expressed endogenous flavin as its chromophore.

### *The LOV domains*

The LOV sensory domains from several different organisms have been successfully used as optogenetic tools. They are all sensitive to blue light (440–473 nm) and use ubiquitously expressed endogenous flavin as a chromophore. The LOV systems differ in how each one uses the light-induced conformational change to regulate cell signalling. One approach directly fuses the LOV domain to an effector protein and relies on the light-induced conformational change in the LOV domain to relieve the autoinhibition<sup>14</sup>. In some optogenetic LOV systems, the LOV domains heterodimerize with natural or engineered binding partners to recruit signalling domains<sup>15</sup>, whereas in other systems the domains homodimerize and bind to DNA, thereby regulating gene expression<sup>33,34</sup>.

### *The Dronpa protein*

Dronpa is a well-known photoactivatable fluorescent protein. Photoactivation not only changes the fluorescence of Dronpa but also changes its quaternary structure. In the 'dark state' (that is, not photoactivated) Dronpa exists as a monomer, and in the fluorescent state it exists as a dimer. As Dronpa has a low affinity for itself in the dimjeric state, the system is most robustly used by fusing a copy of Dronpa to the amino and carboxyl termini of a protein of interest. When Dronpa is activated with light at a wavelength of 390 nm, the Dronpa domains at either end bind to each other, which inhibits the function of the protein of interest by obscuring or altering the active conformation. The extent of protein inhibition can be tracked by the accompanying increase in Dronpa fluorescence. This change can be reversed with light at a wavelength of 490 nm, which converts Dronpa back to a monomer<sup>19</sup>. The system requires no small-molecule chromophore.

## Optogenetic control of cell signalling

There are five general strategies to manipulate intracellular signals with optogenetic proteins (FIG. 1).

### *Inducible protein associations*

The most widely used strategy of manipulating intra-cellular signals using optogenetics takes advantage of light-induced conformational changes to promote the association of two polypeptides. These changes typically cause heterodimerization of a light-responsive protein and its effector. Signalling proteins can be either recruited to or away from their normal site of action, thereby activating or inhibiting intracellular signals (FIG. 1a). The advantage of this technique is that it quickly initiates or terminates signalling and that it is adaptable to many applications. Protein associations and dissociations, and changes in protein localization are ubiquitous modes of regulating cell signalling, and many cellular events have been brought under optogenetic control by exploiting these features. Examples include: CRY2–CIB-based regulation of inositol polyphosphate 5-phosphatase OCRL<sup>35</sup>, PI3K<sup>35</sup> and RAF<sup>36</sup>; the PHYB–Pif-based regulation of actin polymerization<sup>37</sup>, cyclins<sup>38</sup>, CDC42 (REF. 18), lac signalling<sup>38</sup>, PI3K39, RAC<sup>18</sup>, RAS<sup>40</sup> and RHO<sup>18</sup>; and the LOV domain heterodimerization-based regulation of CDC42 and MAPK<sup>15</sup>. A limitation of the heterodimerization-based approach is that the involvement of additional proteins increases the complexity of system optimization.

### *Gene expression*

Cell signalling can also be induced by controlling the expression of a gene of interest. Heterodimerization strategies using CRY2–CIB<sup>10,41</sup>, PHYB–Pif<sup>17</sup> and LOV<sup>42</sup> domains, as well as a LOV-domain-homodimerization approach<sup>33,34</sup>, have successfully regulated transcription by localizing a transcriptional activator to a promoter (FIG. 1b). Other means of protein expression that can be modulated by optogenetics include Cre–loxP-based recombination<sup>10</sup>, chromatin modifications<sup>41</sup>, splicing<sup>43</sup> and translation<sup>44</sup>. An advantage is

that new pathways can be brought under optogenetic control by simply changing the coding sequence of the expressed protein in the DNA. However, regulating the synthesis of signalling proteins may not be fast enough to study many post-translational signalling pathways.

#### *Clustering-based activation*

Some proteins oligomerize in response to light, and this can be used to drive the clustering of signalling proteins that are required in high local concentrations to activate signalling cascades (FIG. 1c). This technique has been used for cryptochrome-based regulation of  $\beta$ -catenin and RHO in the context of transcription and cytoskeletal rearrangements, respectively<sup>11</sup>. A downside of this strategy is that it can be difficult to quantify the number of molecules in the induced clusters, so measuring the strength of the optogenetic input can be challenging, particularly in real time.

#### *Sequestration-based inhibition*

Alternatively, similar to the use of organelle-based recruitment, clustering can be used to sequester proteins away from their site of action<sup>38</sup> (FIG. 1d). This technique has recently been used to inhibit several actin cytoskeleton regulators and as a general technique to regulate signalling proteins fused to GFP<sup>45</sup>. Sequestration is potentially a very general approach, because one only needs to recruit a protein away from its site of action rather than rely on the natural propensity of a protein to signal when clustered.

#### *Intramolecular control of protein function*

Finally, light can be used to induce an intra-molecular conformational change to generate an active signalling protein (FIG. 1e). This technique has been used in conjunction with LOV domains to regulate

CDC42 and RAC<sup>14</sup>, and formins<sup>46</sup> in the context of cell migration, in association with degrons to regulate protein degradation<sup>47</sup> and in conjunction with Dronpa to regulate CDC42 and proteinase K<sup>19</sup>. The advantage of this approach is that it only requires the expression of one protein. It is also one of the few optogenetic approaches that does not involve transcription or light-sensitive ion channels and that has been used in multicellular organisms<sup>48,49</sup>. One of the limitations of this strategy is that intra-molecular inhibition can be challenging to engineer. As a consequence, fewer tools have been developed for this approach than for the more general dimerization-based techniques.

These are the five common ways in which reversible optogenetic protein systems have been used to drive cellular signalling. However, other important differences between optogenetic approaches need to be considered to ensure that the best one is used for a particular experiment.

## Choosing an optogenetic system

There are several considerations when choosing an appropriate optogenetic system. These are summarized in BOX 1 and explained below.

### *Speed of system reversal*

The faster an optogenetic system can be reversed, the more precisely intracellular signals can be manipulated in space and time. Importantly, the rate at which optogenetic systems can be turned off varies by several orders of magnitude, ranging from seconds (for phytochromes inactivated by light), tens of seconds (for LOV domains and Dronpa) and minutes (for CRY2) to hours (for phytochromes inactivated in the dark). Furthermore, some systems such as systems based on LOV domains and CRY2 spontaneously

revert to the dark state, whereas others such as those involving PHYB and Dronpa can be driven to the dark state by separate illumination wavelengths. Light-driven reversal tends to reduce basal activity, expand the dynamic range and offer faster turn-off times of optogenetic systems. Faster turn-off rates increase spatial control, as the activated molecule cannot diffuse far from the excitatory light before it is turned off.

### *Quantifying the input*

Using optogenetic tools for more than qualitative experiments requires not only a means to quantify the dose of activating light but also a way to quantify the strength of the optogenetic input — that is, the amount of optogenetic proteins that are actively signalling. Owing to non-linearities in these systems, reducing the intensity or duration of activating light by 50% does not necessarily decrease the amount of the signalling complex formed to the same degree. Quantification is easiest with two-component optogenetic systems that regulate protein recruitment to the plasma membrane, in which changes in the localization of the signalling domain of interest can be analysed by fusing it to a fluorescent protein. For example, membrane recruitment of a fluorescently tagged PI3K subunit was used to quantify the strength of optogenetic activation of this enzyme<sup>50</sup>. Single-component systems typically require a live-cell reporter immediately downstream of the input to quantify the strength of optogenetic activation. An interesting exception is the Dronpa system. When used to intra-molecularly inhibit a protein, Dronpa ‘dims’ when converted to the signalling competent, monomeric state. Thus, it is important to note that evaluating intermediate levels of Dronpa activation requires the measurement of dim fluorescence on a light background.

### *Considering dynamic range*

Optogenetic systems markedly vary in their dynamic range, which is typically a function of two parameters: the basal activation of the system and the affinity of the photoproteins for their binding partners. Higher dynamic ranges are preferable for manipulating cell signalling cascades over a wide range of expression levels of the optogenetic components. Cryptochrome- and LOV-domain-based systems have higher basal activation than systems involving PHYB and Dronpa, both of which can be forced into the off state through illumination with inactivating wavelengths. The affinity of photoproteins for their binding partners varies by several orders of magnitude from 100 nM (estimated PHYB–Pif6 affinity in cells)<sup>18</sup>, to 600 nM (measured PHYB–Pif3 affinity in vitro)<sup>37</sup> to 10  $\mu$ M (for Dronpa oligomerization)<sup>19</sup>. Taken together, the largest dynamic range is expected for the phytochrome system.

### *Ease of titration*

The ease with which an input can be titrated to and maintained at a desired level (something that is necessary for analysing the equilibrium of cell signalling) depends on how quickly the system turns off. Producing stable, intermediate levels of a signal in systems that take minutes (rather than seconds) to turn off can be challenging and requires the level of activating light to be carefully controlled to counteract spontaneous inactivation. It is easiest to achieve a stable, intermediate amount of signalling complexes with the PHYB- and Dronpa-based systems, because they can turn off in seconds and can be actively inhibited with light, whereas the CRY2- and LOV-domain-based systems spontaneously revert. Thus, constant illumination with a fixed ratio of stimulatory light to inhibitory light can keep an input at a desired level. Furthermore, the fact that stimulatory and inhibitory light buffer each other can overcome the effects of incidental excitation that can occur while imaging other chromophores.



### *Chromophore requirement*

Optogenetic proteins that use an endogenous chromophore, such as CRY2, LOV domains and Dronpa, are well suited for multicellular and developmental models, in which the delivery of an exogenous chromophore may be impractical. Although some progress has been made in synthesizing chromophores in situ for bacterial and mammalian cells in culture by co-expressing the appropriate enzymes from plants and algae<sup>30,31</sup>, this has not yet been demonstrated for multicellular organisms. In some contexts, such as when controlling irreversible pathways (for example, differentiation or apoptosis)<sup>51</sup>, having the system only respond to light upon the addition of an exogenous chromophore may be an advantage to limit the activation of a 'leaky' pathway.

### *Compatibility with fluorescent reporters*

Finally, optogenetic inputs should ideally be paired with some way of measuring both the strength of the optogenetically induced signal and the activity of a live-cell reporter of the resulting downstream response. Such reporters frequently involve the use of fluorescent proteins, and it is important to know which ones can be safely imaged without activating the optogenetic input. Luckily, most optogenetic systems include at least two 'safe' spectra of wavelengths that can be imaged without markedly altering the activation of the system. For example, when investigating how son of sevenless (Sos; a RAS guanine nucleotide-exchange factor (GEF)) activates Erk, light at a wavelength of 514 nm was used to measure Pif–YFP–Sos recruitment to the plasma membrane (the input); and light at a wavelength of 405 nm was used to measure how the cell responded to Pif–YFP–Sos recruitment by tracking Erk–blue fluorescent protein translocation into the nucleus<sup>40</sup>. Cells exposed to light at wavelengths of 514 nm and 405 nm are safe, because these wavelengths do not markedly alter the PHYB–Pif interaction<sup>39</sup>.

### *Optogenetic hardware*

As the discussed optogenetic systems are fairly sensitive to visible light, various common light sources on a microscope can activate them. Epifluorescent light, FRAP (fluorescence recovery after photobleaching) lasers with the power turned to a minimum, light-emitting diodes and even glass filters in the bright-field path have activated these optogenetic systems. The intensity of light from light-emitting diodes and some laser sources can be continuously varied, which makes them ideal for precisely titrating an optogenetic input or maintaining it at a specific level with feedback control<sup>39</sup>.

These light sources can be spatially restricted by closing down the corresponding field diaphragm. Single cells can be stimulated with a low magnification objective, whereas subcellular regions can be activated with a high magnification objective. Finer spatial control requires a digital micromirror device, an array of tiled mirrors that can be individually toggled to project an arbitrary pattern of light. Using a digital micromirror device, exact regions of a cell can be targeted (for example, just the dendrites of a neuron) or the pattern of illumination can be updated as the cell changes shape. Some FRAP systems already use a digital micromirror device and can be co-opted for optogenetic experiments once the power is greatly reduced.

### Quantifying signal integration

Optogenetic tools strongly synergize with existing biological approaches. Biochemistry and genetics are often used to first identify signalling molecules and to discern how they activate and inhibit one another. However, assessing how these individual components are linked together to generate complex cellular behaviours can be much more challenging. In some instances, loss-of-function perturbations of single nodes in a pathway simply break a signalling circuit and are insufficient for understanding how each node

functions in the overall network. Similarly, not all pathways are sufficiently understood to enable their full biochemical reconstitution, and even those that are well understood may exhibit different behaviours in vitro than in the cell.

For pathways that are sufficiently understood to enable signalling nodes to be manipulated by precise optogenetic inputs, it is now possible to carry out in vivo biochemical experiments<sup>52</sup> to understand the function of individual subcircuits within complex signalling networks. Optogenetics can be used to both isolate distinct subcircuits and determine their logic of signal integration<sup>40</sup>.

#### *Isolating distinct subcircuits*

The easiest way to modify signalling cascades is by the addition of extracellular ligands, but activating cellular receptors induces many arms of a signalling pathway. These arms often interact with one another in a complex manner that may be difficult to disentangle when analysed as a whole. Optogenetic inputs can be used to manipulate downstream nodes in signalling cascades, thereby breaking down a large, complex pathway into a series of smaller, easier-to-understand units (FIG. 2a).

#### *Single-cell dose–response curves*

Just as one can tell whether an enzyme functions in a cooperative manner in vitro by varying the amount of enzyme and measuring the resulting product, it is also possible to determine whether a part of a pathway functions in a graded or switch-like manner in vivo by varying the amount of upstream input and measuring the downstream response. Importantly, the speed and reversibility of optogenetic systems make it possible to generate dose–response curves for individual cells. It is well appreciated that

population-level analysis tools such as western blotting obscure single-cell behaviours and give overall averages that can lead to incorrect conclusions regarding individual cell behaviour<sup>53</sup>. Single-cell analyses are preferable, but these are commonly implemented through techniques such as flow cytometry. Using this method, one datum is acquired per cell, and the overall population of individual cells is used to build a response curve. This has the disadvantage that cell-to-cell variability can obscure the true response of signalling cascades. Indeed, single-cell dose–response curves generated using optogenetics — for instance, by measuring the concentration of light-gated SOS (a RAS activator) versus the concentration of ERK (a RAS effector) — show marked smaller variability than generating a response curve using the entire cell population<sup>40</sup> (FIG. 2b). Optogenetics can also be used in conjunction with pharmacological approaches to analyse the input–output behaviour of a signalling node before and after drug treatment, which overcomes the confounding effects of cell variability by using each cell as its own control (for example, fibroblast cells before and after treatment with PI3K inhibitors)<sup>39</sup> (FIG. 2c).

The x axis for these single-cell dose–response curves is not restricted to the concentration of the signalling input. As optogenetic signals can be varied and measured in space and time, as well as in concentration, we can also analyse the cell response to the rate of change of the input<sup>54</sup>, the fold change of the input<sup>55,56</sup>, the spatial distribution of the input<sup>57</sup>, and so on (FIG. 2d). All of these signalling attributes have been found to be important in different biological contexts.

### Optogenetic control of signals in space

The spatial control of cell signalling has a fundamental role in cell and organismal biology. To understand these processes, we need tools to actively manipulate signals in space, both at the level of individual cells in organisms and on a subcellular level.

### *Spatial regulation of multicellular signalling*

Communication between cells can enable a group of cells to more sensitively interpret signals than cells acting alone. A classic example is visual gradient interpretation in the horseshoe crab. By spatially restricting light to only two light-sensitive cells at a time, two rules for contrast enhancement were derived<sup>58</sup>: a stronger external stimulus causes a stronger upstream signal; and the stronger the upstream signal, the stronger the inhibitory effect of the cell on its neighbours (FIG. 3a).

During visual contrast enhancement, although all cells inhibit the activity of each other to some extent, cells in the brightest areas reduce the activity of their neighbour the most, which emphasizes slight differences in an external gradient. This so-called lateral inhibition functions in the eyes, from horseshoe crabs to humans, and increases the contrast in our vision before action potentials enter the optic nerve.

More recently, optogenetic approaches have shown how cellular comparison can sharpen signal interpretation in other multicellular contexts. In *Drosophila melanogaster*, small groups of border cells collectively migrate about 175  $\mu\text{m}$  up a chemical gradient to a maturing oocyte in the egg chamber<sup>48</sup>. This collection of cells uses lateral inhibition to ensure that only the one or two cells at the highest point in the gradient actively protrude. Using photoactivatable Rac to override normal chemotactic cues and initiate movement in cells at the side of the collective caused the normally leading cells to stop protruding. Thus, the activity of one cell inhibits the activity of its neighbour. Although all of the border cells are capable of protrusion, lateral inhibition ensures that only one or two leading cells are active at a time and that a collective decision is possible (FIG. 3b).

The rules derived from these two examples show how regulation at a distance increases the ability of a system to properly respond to external cues. They were only discovered because spatially restricted inputs enabled the investigation of how the activity of one cell affects the activity of neighbouring cells. It is probably no coincidence that biology converged on lateral inhibition to increase gradient sensing of both light and chemoattractants.

### *Spatial regulation of subcellular signalling*

On a multicellular level, non-optogenetic tools have been used to study the spatial control of signalling — for instance, the transplantation of cells or the generation of single-cell clones. However, optogenetic tools enable much more precise and dynamic control of cell signalling than non-optogenetic tools. There have been fewer tools to manipulate spatial signals on a subcellular level, and optogenetic systems are enabling some of the first demonstrations of the spatial sufficiency of signals to coordinate cellular processes, including the molecules that direct cell polarization and movement<sup>14,15,18,35,39,49</sup>. For example, LOV-domain-based control of RAC activity showed that asymmetries in the activation of this GTPase are sufficient to specify the migratory direction of individual neutrophils in zebrafish<sup>49</sup> and the collective migration of border cells in *D. melanogaster*<sup>48</sup>.

### Optogenetic control of signals in time

Although some signalling cascades only respond to the current level of stimulus, other cascades respond to the timing of the input<sup>59</sup>. For example, adaptive cascades, like most sensory inputs, reset themselves to the current level of stimulus and primarily sense changes in, as opposed to absolute levels of, signalling

inputs<sup>54</sup>. Other cascades seem to monitor the dynamics of the input. For example, sustained or transient pathway activity can drive different cellular decisions. Differences in the duration of MAPK signalling can regulate whether cells decide to proliferate or differentiate<sup>60</sup>, whereas differences in the signal duration of the tumour suppressor protein p53 can regulate whether cells arrest their cell cycle or apoptose<sup>61</sup>. In this section, we address the challenges in analysing these processes together with the opportunities that optogenetic systems present for probing the role of timing in cell decisions.

The dynamics of intracellular signalling has been implicated in the regulation of cellular decisions. For example, different ligands trigger different dynamics of ERK activation (epidermal growth factor (EGF) drives transient ERK activation, whereas nerve growth factor (NGF) drives sustained ERK activation), and these different dynamics correlate with different downstream responses (EGF drives the proliferation of PC12 cells, whereas NGF drives the differentiation of PC12 cells). To investigate whether differences in the timing of MAPK activation are causative for downstream behaviours, one group used pharmacological activators and inhibitors of protein kinase C to produce sustained activation of MAPK in response to EGF and transient activation of MAPK in response to NGF<sup>60</sup>. Exchanging the MAPK dynamics downstream of these ligands also exchanged their downstream responses, which is consistent with the idea that the timing of MAPK activation determines the resulting cellular outcome (FIG. 4a). As many signalling cascades are not sufficiently understood to use pharmacological or genetic means to influence intracellular signalling dynamics, and because these pharmacological perturbations also affect the topology of the signalling network, it would be preferable to directly manipulate intracellular signalling dynamics in a user-defined manner. This is now possible with optogenetic inputs, and multiple groups have used this approach to demonstrate that the MAPK signal duration is sufficient to regulate the differentiation decision in PC12 cells<sup>40,62</sup> and to identify the signalling pathways that are differentially activated by sustained versus transient MAPK activation<sup>40</sup> (FIG. 4b).

## Conclusions and perspectives

Optogenetic systems have moved beyond the control of light-gated ion channels to include a wide range of other light-responsive proteins and cellular pathways that can now be manipulated by light. All of these systems started with proof-of-principle demonstrations, activating signalling pathways that others had previously activated by protein overexpression, microinjection, and so on. However, investigators have recently taken advantage of the capacity of optogenetics to dynamically manipulate and measure signals in space and time to address questions that have been difficult or impossible to address with other tools.

We end with a wish list for the field. The optogenetics field is based on light-responsive proteins from plants and other systems. We are fortunate that these systems work as well as they do, but we should consider them like the first generation of GFPs — systems with a huge potential to evolve and to be optimized. Some engineering work has been done for the LOV domains, but far more work could be done to optimize the affinities, the photoactivation and photoreversion rates, the wavelengths for photoswitching and the light sensitivity of other systems. This optimization will be aided by advances in the structure and mechanism of these photosensors<sup>63,69</sup>. Furthermore, we would like these systems to be completely orthogonal to cell signalling cascades, but we do not yet know whether post-translational modifications affect their function in optogenetic applications. To understand these constraints, it will be useful to follow advances in the physiology and regulation of these proteins in their normal context<sup>64-66</sup>. On a similar note, many of these proteins were chosen for their light-responsive interactions in plants, and a greater understanding of their regulators could expand our strategies for photoregulation. For instance, cryptochromes not only form heterodimers with downstream effectors in response to light (such as CIB1)<sup>9</sup> but also oligomerize in response to light<sup>32</sup>. Both of these properties have been used to regulate



cell signalling<sup>10,11</sup>, and a greater knowledge of phototransduction mechanisms is likely to reveal more surprises and opportunities for optogenetics.

## Acknowledgments

The authors thank members of the Weiner laboratory for helpful discussions. This work was supported by a Genentech Fellowship (D.T.) and US National Institutes of Health (NIH) grants GM084040, GM096164 and GM109899 (O.D.W.).

## Footnotes

### Competing interests statement

The authors declare no competing interests.

## References

1. Kaplan JH, Forbush B, Hoffman JF. Rapid photolytic release of adenosine 5-triphosphate from a protected analogue: utilization by the Na:K pump of human red blood cell ghosts. *Biochemistry*. 1978;17:1929–1935.
2. Callaway EM, Katz LC. Photostimulation using caged glutamate reveals functional circuitry in living brain slices. *Proc Natl Acad Sci USA*. 1993;90:7661–7665.
3. Zemelman BV, Lee GA, Ng M, Miesenbock G. Selective photostimulation of genetically chARGed neurons. *Neuron*. 2002;33:15–22.

4. Boyden ES, Zhang F, Bamberg E, Nagel G, Deisseroth K. Millisecond-timescale, genetically targeted optical control of neural activity. *Nature Neurosci.* 2005;8:1263–1268.
5. Li X, et al. Fast noninvasive activation and inhibition of neural and network activity by vertebrate rhodopsin and green algae channelrhodopsin. *Proc Natl Acad Sci USA.* 2005;102:17816–17821.
6. Zhang F, et al. Multimodal fast optical interrogation of neural circuitry. *Nature.* 2007;446:633–639.
7. Arrenberg AB, Stainier DY, Baier H, Huisken J. Optogenetic control of cardiac function. *Science.* 2010;330:971–974.
8. Tsai HC, et al. Phasic firing in dopaminergic neurons is sufficient for behavioral conditioning. *Science.* 2009;324:1080–1084.
9. Liu H, et al. Photoexcited CRY2 interacts with CIB1 to regulate transcription and floral initiation in *Arabidopsis*. *Science.* 2008;322:1535–1539.
10. Kennedy MJ, et al. Rapid blue-light-mediated induction of protein interactions in living cells. *Nature Methods.* 2010;7:973–975.
11. Bugaj LJ, Choksi AT, Mesuda CK, Kane RS, Schaffer DV. Optogenetic protein clustering and signaling activation in mammalian cells. *Nature Methods.* 2013;10:249–252.
12. Christie JM, Salomon M, Nozue K, Wada M, Briggs WR. LOV (light, oxygen, or voltage) domains of the blue-light photoreceptor phototropin (*nph1*): binding sites for the chromophore flavin mononucleotide. *Proc Natl Acad Sci USA.* 1999;96:8779–8783.
13. Harper SM, Neil LC, Gardner KH. Structural basis of a phototropin light switch. *Science.* 2003;301:1541–1544.

14. Wu YI, et al. A genetically encoded photoactivatable Rac controls the motility of living cells. *Nature*. 2009;461:104–108.
15. Strickland D, et al. TULIPs: tunable, light-controlled interacting protein tags for cell biology. *Nature Methods*. 2012;9:379–384.
16. Ni M, Tepperman JM, Quail PH. Binding of phytochrome B to its nuclear signalling partner Pif3 is reversibly induced by light. *Nature*. 1999;400:781–784.
17. Shimizu-Sato S, Huq E, Tepperman JM, Quail PH. A light-switchable gene promoter system. *Nature Biotech*. 2002;20:1041–1044.
18. Levskaya A, Weiner OD, Lim WA, Voigt CA. Spatiotemporal control of cell signalling using a light-switchable protein interaction. *Nature*. 2009;461:997–1001.
19. Zhou XX, Chung HK, Lam AJ, Lin MZ. Optical control of protein activity by fluorescent protein domains. *Science*. 2012;338:810–814.
20. Ando R, Mizuno H, Miyawaki A. Regulated fast nucleocytoplasmic shuttling observed by reversible protein highlighting. *Science*. 2004;306:1370–1373.
21. Fenno L, Yizhar O, Deisseroth K. The development and application of optogenetics. *Annu Rev Neurosci*. 2011;34:389–412.
22. Ryu MH, Moskvin OV, Siltberg-Liberles J, Gomelsky M. Natural and engineered photoactivated nucleotidyl cyclases for optogenetic applications. *J Biol Chem*. 2010;285:41501–41508.
23. Stierl M, et al. Light modulation of cellular cAMP by a small bacterial photoactivated adenylyl cyclase, bPAC, of the soil bacterium *Beggiatoa*. *J Biol Chem*. 2011;286:1181–1188.

24. Airan RD, Thompson KR, Fenno LE, Bernstein H, Deisseroth K. Temporally precise in vivo control of intracellular signalling. *Nature*. 2009;458:1025–1029.
25. Karunaratne WK, Giri L, Patel AK, Venkatesh KV, Gautam N. Optical control demonstrates switch-like PIP3 dynamics underlying the initiation of immune cell migration. *Proc Natl Acad Sci USA*. 2013;110:E1575–E1583.
26. Chen D, Gibson ES, Kennedy MJ. A light-triggered protein secretion system. *J Cell Biol*. 2013;201:631–640.
27. Crefcoeur RP, Yin R, Ulm R, Halazonetis TD. Ultraviolet-B-mediated induction of protein–protein interactions in mammalian cells. *Nature Commun*. 2013;4:1779.
28. Yazawa M, Sadaghiani AM, Hsueh B, Dolmetsch RE. Induction of protein-protein interactions in live cells using light. *Nature Biotech*. 2009;27:941–945.
29. Bongers KM, Rakhit R, Payumo AY, Chen JK, Wandless TJ. General method for regulating protein stability with light. *ACS Chem Biol*. 2014;9:111–115.
30. Gambetta GA, Lagarias JC. Genetic engineering of phytochrome biosynthesis in bacteria. *Proc Natl Acad Sci USA*. 2001;98:10566–10571.
31. Muller K, et al. Synthesis of phycocyanobilin in mammalian cells. *Chem Commun (Camb)* 2013;49:8970–8972.
32. Mas P, Devlin PF, Panda S, Kay SA. Functional interaction of phytochrome B and cryptochrome 2. *Nature*. 2000;408:207–211.
33. Wang X, Chen X, Yang Y. Spatiotemporal control of gene expression by a light-switchable transgene system. *Nature Methods*. 2012;9:266–269.

34. Motta-Mena LB, et al. An optogenetic gene expression system with rapid activation and deactivation kinetics. *Nature Chem Biol.* 2014;10:196–202.
35. Idevall-Hagren O, Dickson EJ, Hille B, Toomre DK, De Camilli P. Optogenetic control of phosphoinositide metabolism. *Proc Natl Acad Sci USA.* 2012;109:E2316–E2323.
36. Wend S, et al. Optogenetic control of protein kinase activity in mammalian cells. *ACS Synth Biol.* 2013;3:280–285.
37. Leung DW, Otomo C, Chory J, Rosen MK. Genetically encoded photoswitching of actin assembly through the Cdc42–WASP–Arp2/3 complex pathway. *Proc Natl Acad Sci USA.* 2008;105:12797–12802.
38. Yang X, Jost AP, Weiner OD, Tang C. A light-inducible organelle targeting system for dynamically activating and inactivating signaling in budding yeast. *Mol Biol Cell.* 2013;24:2419–2430.
39. Toettcher JE, Gong D, Lim WA, Weiner OD. Light-based feedback for controlling intracellular signaling dynamics. *Nature Methods.* 2011;8:837–839.
40. Toettcher JE, Weiner OD, Lim WA. Using optogenetics to interrogate the dynamic control of signal transmission by the Ras/Erk module. *Cell.* 2013;155:1422–1434.
41. Konermann S, et al. Optical control of mammalian endogenous transcription and epigenetic states. *Nature.* 2013;500:472–476.
42. Lungu OI, et al. Designing photoswitchable peptides using the AsLOV2 domain. *Chem Biol.* 2012;19:507–517.
43. Tyszkiewicz AB, Muir TW. Activation of protein splicing with light in yeast. *Nature Methods.* 2008;5:303–305.

44. Cao J, et al. Light-inducible activation of target mRNA translation in mammalian cells. *Chem Commun.* 2013;49:8338–8340.
45. Lee S, et al. Reversible protein inactivation by optogenetic trapping in cells. *Nature Methods.* 2014;11:633–636.
46. Rao MV, Chu PH, Hahn KM, Zaidel-Bar R. An optogenetic tool for the activation of endogenous diaphanous-related formins induces thickening of stress fibers without an increase in contractility. *Cytoskeleton.* 2013;70:394–407.
47. Renicke C, Schuster D, Usherenko S, Essen LO, Taxis C. A LOV2 domain-based optogenetic tool to control protein degradation and cellular function. *Chem Biol.* 2013;20:619–626.
48. Wang X, He L, Wu YI, Hahn KM, Montell DJ. Light-mediated activation reveals a key role for Rac in collective guidance of cell movement in vivo. *Nature Cell Biol.* 2010;12:591–597.
49. Yoo SK, et al. Differential regulation of protrusion and polarity by PI3K during neutrophil motility in live zebrafish. *Dev Cell.* 2010;18:226–236.
50. Toettcher JE, Gong D, Lim WA, Weiner OD. Light control of plasma membrane recruitment using the Phy–Pif system. *Methods Enzymol.* 2011;497:409–423.
51. Spencer SL, Gaudet S, Albeck JG, Burke JM, Sorger PK. Non-genetic origins of cell-to-cell variability in TRAIL-induced apoptosis. *Nature.* 2009;459:428–432.
52. Haber JE. In vivo biochemistry: physical monitoring of recombination induced by site-specific endonucleases. *Bioessays.* 1995;17:609–620.
53. Ferrell JE, Jr, Machleder EM. The biochemical basis of an all-or-none cell fate switch in *Xenopus* oocytes. *Science.* 1998;280:895–898.

54. Shimizu TS, Tu Y, Berg HC. A modular gradient-sensing network for chemotaxis in *Escherichia coli* revealed by responses to time-varying stimuli. *Mol Syst Biol.* 2010;6:382.
55. Goentoro L, Shoval O, Kirschner MW, Alon U. The incoherent feedforward loop can provide fold-change detection in gene regulation. *Mol Cell.* 2009;36:894–899.
56. Wartlick O, et al. Dynamics of Dpp signaling and proliferation control. *Science.* 2011;331:1154–1159.
57. Devreotes PN, Zigmond SH. Chemotaxis in eukaryotic cells: a focus on leukocytes and *Dictyostelium*. *Annu Rev Cell Biol.* 1988;4:649–686.
58. Hartline HK, Wagner HG, Ratliff F. Inhibition in the eye of *Limulus*. *J Gen Physiol.* 1956;39:651–673.
59. Purvis JE, Lahav G. Encoding and decoding cellular information through signaling dynamics. *Cell.* 2013;152:945–956.
60. Santos SD, Verveer PJ, Bastiaens PI. Growth factor-induced MAPK network topology shapes Erk response determining PC-12 cell fate. *Nature Cell Biol.* 2007;9:324–330.
61. Purvis JE, et al. p53 dynamics control cell fate. *Science.* 2012;336:1440–1444.
62. Zhang K, et al. Light-mediated kinetic control reveals the temporal effect of the Raf/MEK/ERK pathway in PC12 cell neurite outgrowth. *PLoS ONE.* 2014;9:e92917.
63. Takala H, et al. Signal amplification and transduction in phytochrome photosensors. *Nature.* 2014;509:245–248.
64. Kim JI, et al. Phytochrome phosphorylation modulates light signaling by influencing the protein–protein interaction. *Plant Cell.* 2004;16:2629–2640.
65. Medzihradzky M, et al. Phosphorylation of phytochrome B inhibits light-induced signaling via accelerated dark reversion in *Arabidopsis*. *Plant Cell.* 2013;25:535–544.

66. Hughes RM, Vrana JD, Song J, Tucker CL. Light-dependent, dark-promoted interaction between Arabidopsis cryptochrome 1 and phytochrome B proteins. *J Biol Chem.* 2012;287:22165–22172.
67. Strickland D, et al. Rationally improving LOV domain-based photoswitches. *Nature Methods.* 2010;7:623–626.
68. Loewer A, Karanam K, Mock C, Lahav G. The p53 response in single cells is linearly correlated to the number of DNA breaks without a distinct threshold. *BMC Biol.* 2013;11:114.
69. Burgie ES, Bussell AN, Walker JM, Dubiel K, Vierstra RD. Crystal structure of the photosensing module from a red/far-red light-absorbing plant phytochrome. *Proc Natl Acad Sci USA.* (in the press)



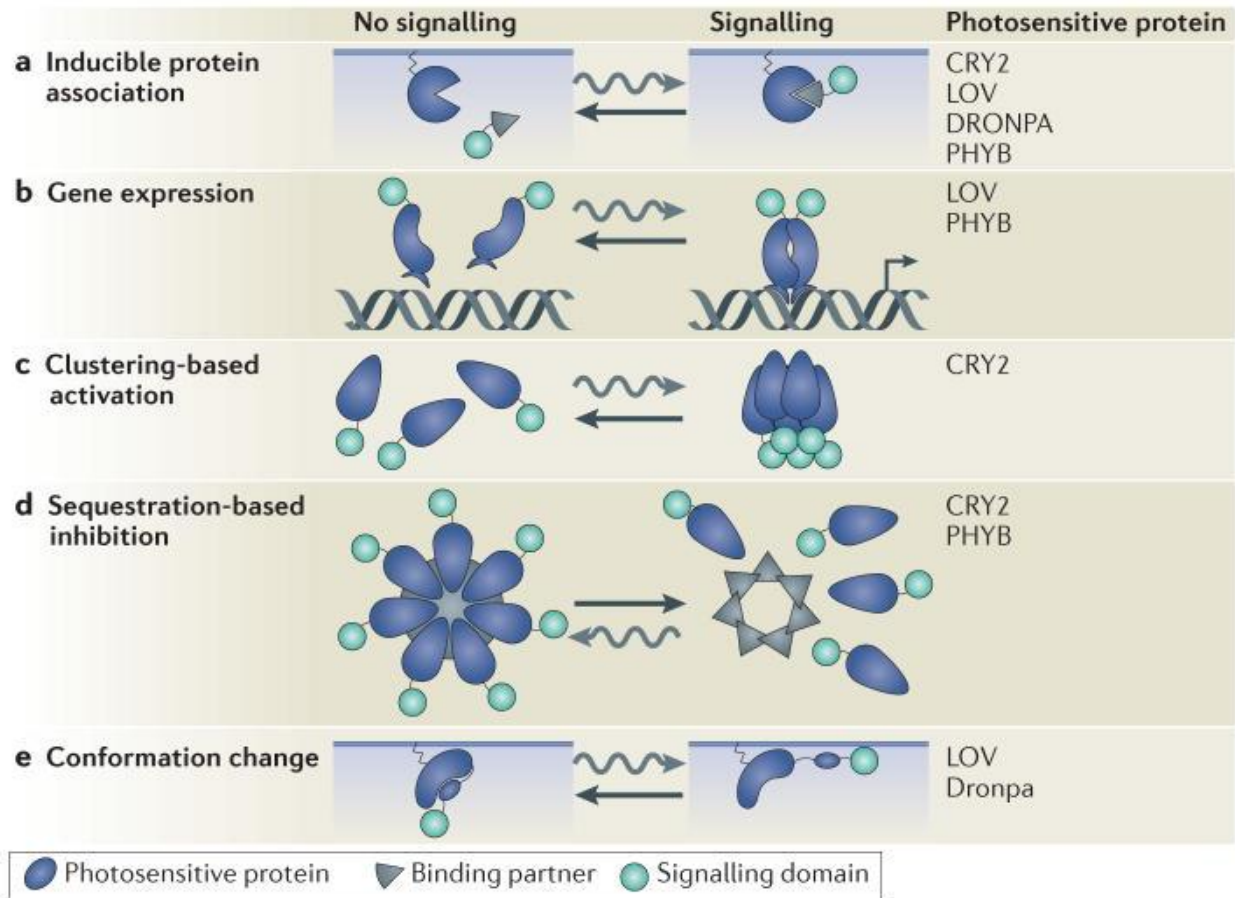


Figure 1: Different strategies for optogenetic inputs

Optogenetically stimulated signals can be induced in various ways (the photosensitive proteins that have been used for each approach are listed). System reversion occurs either in the dark or can be stimulated with light depending on the system used (BOX 1). a | Heterodimerization is used to recruit a signalling domain to its substrate, which is commonly located on the plasma membrane. b | Homodimerization and heterodimerization techniques recruit transcriptional activators or other DNA-modifying proteins to the DNA to initiate the expression of a gene of interest. c | CRYPTOCHROME 2 (CRY2) naturally clusters when it is activated. By fusing CRY2 with signalling domains, the activities of which depend on domain density, signalling can be activated with light. d | Alternatively, signalling can be inhibited by sequestering a signalling protein away from its site of action. Proteins can be sequestered in cytosolic clusters or recruited

to compartments away from their downstream effectors or upstream activators. e | Conformational changes in the photosensitive protein can expose a concealed signalling domain or relieve a protein from an allosterically autoinhibited state. LOV, light-oxygen-voltage; PHYB, PHYTOCHROME B. Curvy arrows indicate the response of the system to light, whereas straight arrows indicate dark- or light-stimulated reversion. The small arrow on the DNA represents active transcription.

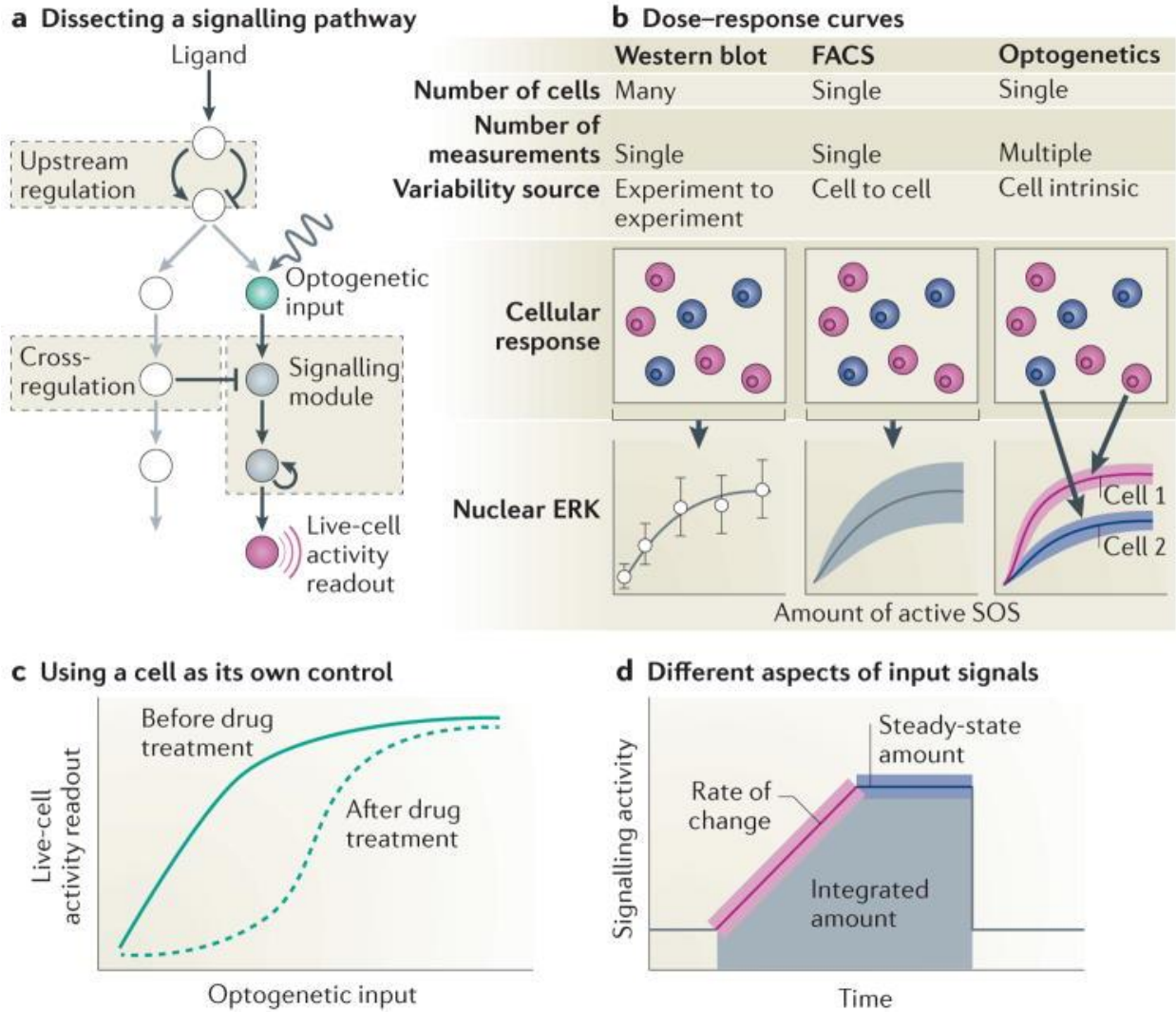


Figure 2: Optogenetics for in vivo biochemistry

a | Assessing the function of an arm of a signalling pathway with precise, defined inputs is difficult with traditional tools, as endogenous ligands frequently activate upstream and parallel regulatory connections in addition to the signalling module under study (grey arrows). Optogenetic inputs circumvent this problem by initiating precise, defined signals at intermediate points in a pathway. By measuring the downstream response of a cell with a live-cell activity reporter, the function of the intervening signalling module can be inferred. b | Dose-response curves generated for a population of cells using western blots obscure single-cell behaviour. Single-cell techniques such as immunolabelling-based fluorescence-

activated cell sorting (FACS) use fixed cells and, as one time point is not sufficient to generate a dose–response curve, the response of thousands of cells must be combined to do so. Cell-to-cell variation confounds the measurement of cell responses because of extrinsic differences in the responses, and the aggregation of data from multiple cells distorts the intrinsic behaviour of the pathway. The titratability, speed and reversibility of optogenetic inputs enable multiple measurements and thus the generation of complete dose–response curves for individual living cells<sup>40</sup>. This approach removes previous noise arising from cell heterogeneity and provides the most detailed view of the intrinsic precision of signalling pathways in living cells. Here, data are shown for light-gated activation of RAS (through PHYTOCHROME B (PHYB)–PHYTOCHROME INTERACTING FACTOR (Pif)-based recruitment of the Ras activator son of sevenless (SOS)) and its induction of ERK activation, as analysed by nuclear recruitment of a fluorescently tagged ERK40. The precision of optogenetic dose–response curves makes them ideal for understanding how a particular enzyme regulates a signalling pathway. c | Beyond determining whether drug treatment blocks a pathway, optogenetics can uncover how co-occurring cellular events regulate core pathways by carrying out several experiments on one cell, which enables it to be used as its own control. For example, kinase phosphorylation of a scaffold may increase protein binding and thus pathway sensitivity. Generating a dose–response curve using optogenetic techniques before and after kinase inhibition by the addition of a drug is a powerful approach for detecting these regulatory effects in a manner that is not confounded by cell-to-cell variation in response. d | Signalling pathways can respond to more than the steady-state amount of a signal, such as its rate of change or integrated amount (sum of input over time). As the optogenetic inputs can be varied in space, time and concentration, many types of input–output analyses can be conducted. All of these signalling attributes have been found to be important in different biological contexts<sup>40,51,54–57,68</sup>. Part b reprinted from Cell, 155/1430, Toettcher, J. E., Weiner, O. D. & Lim, W. A., Using optogenetics to interrogate the dynamic control of signal transmission by the Ras/Erk module, 1422–1434, Copyright (2013), with permission from Elsevier.



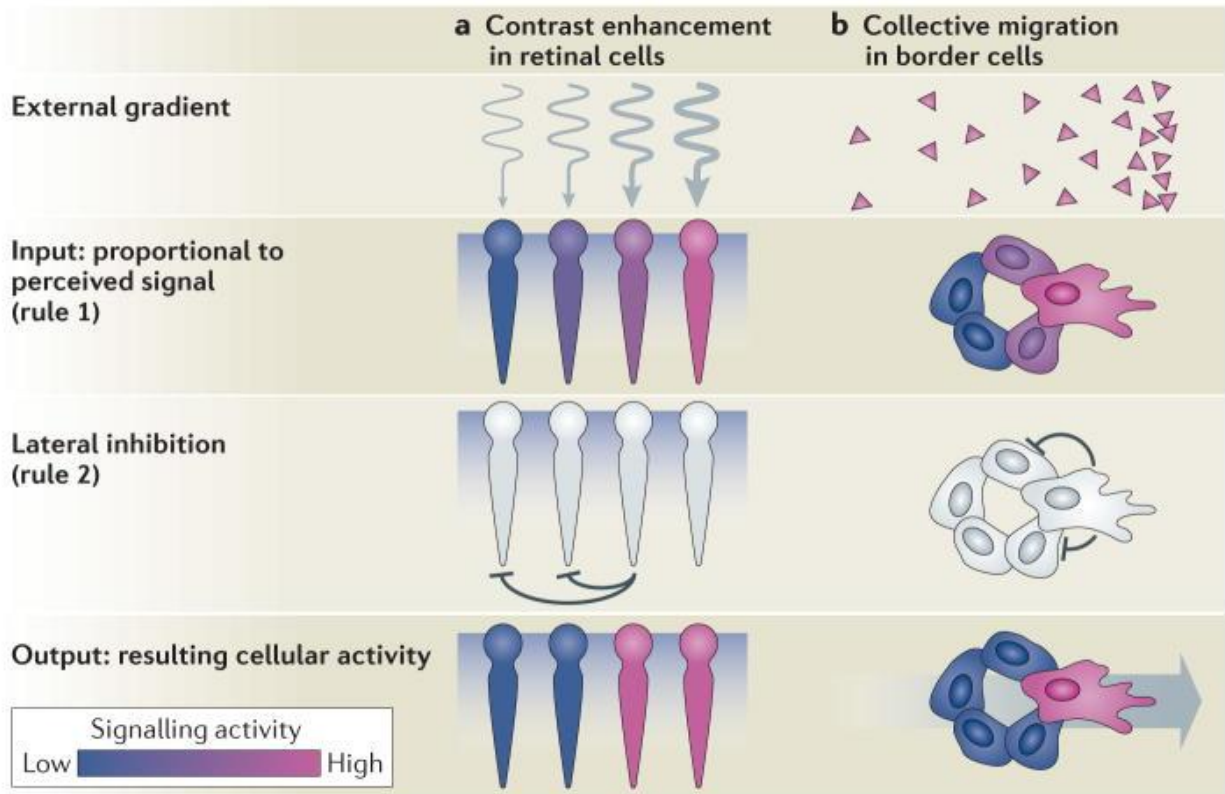


Figure 3: Optogenetic control of signals in space

Both light-sensitive cells in the eye<sup>58</sup> (part a) and groups of chemotactic cells in the *Drosophila melanogaster* egg chamber<sup>48</sup> (part b) use lateral inhibition to generate strong cellular responses from shallow external gradients. Acting alone, each cell can sense the external gradient but by comparing with their neighbours a higher contrast interpretation is possible. First, the cells generate an upstream signal that is proportional to the perceived input (rule 1). Next, cells inhibit the activity of their neighbours: the stronger the perceived signal, the stronger the lateral inhibition (rule 2). The end result is that weak signals are inhibited more than strong ones, which produces an amplified representation of subtle external gradients and enhances visual contrast in the eye (part a). A similar lateral inhibition mechanism is thought to enable coordinated collective cell migration in the fly egg chamber (part b) for the interpretation of external chemoattractant gradients (triangles). Here, the light-controlled activation of Rac inhibits

protrusion in adjacent cells, and the inhibition of Rac in the leader cell activates protrusions in adjacent cells. These dissections of lateral inhibition were only possible, because cells were individually activated with spatially restricted inputs.

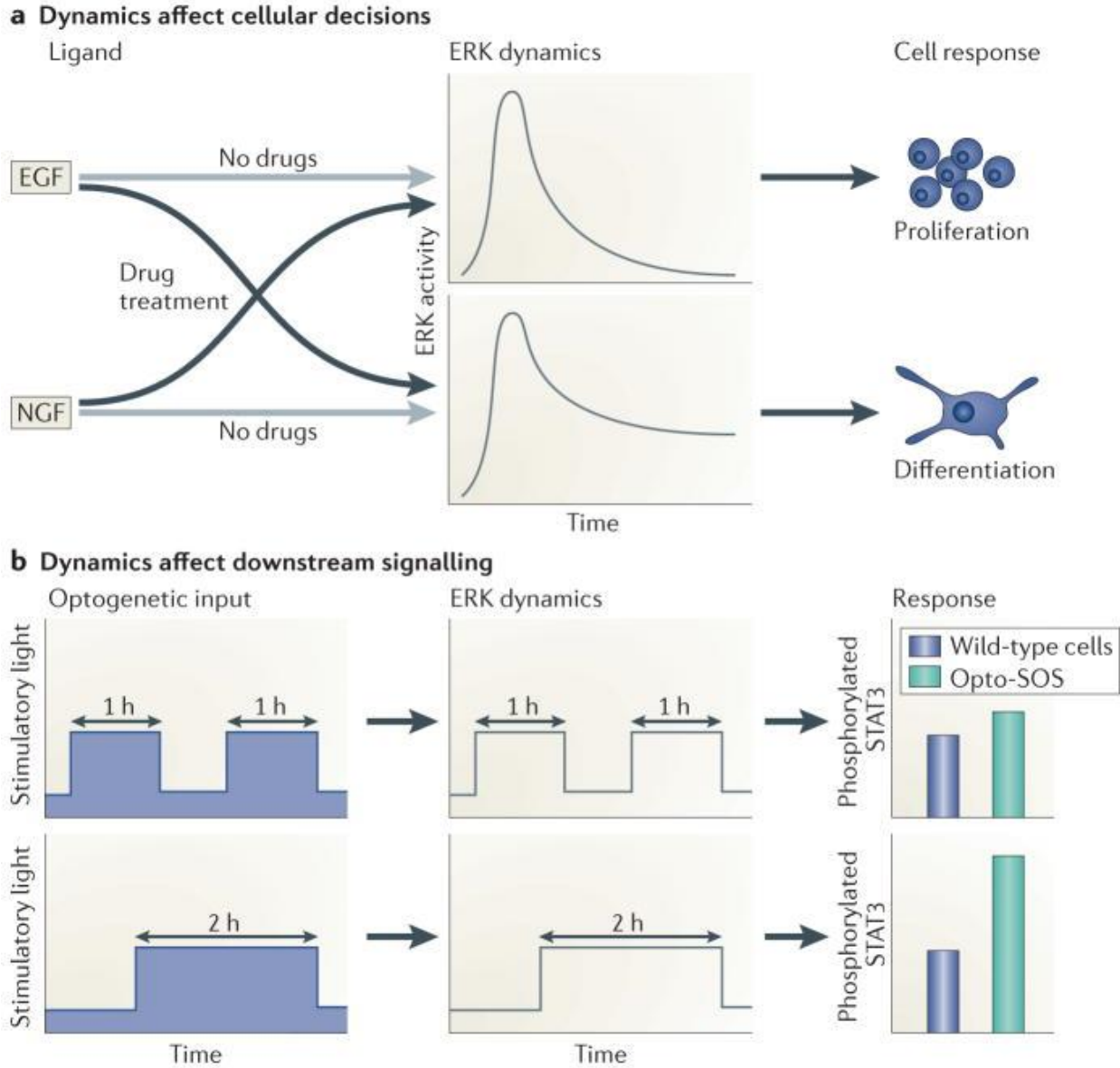


Figure 4: Optogenetic control of signals in time

a | Signalling dynamics can affect cellular decisions. Normally, treatment of PC12 cells with epidermal growth factor (EGF) causes transient ERK activity and cellular proliferation, whereas treatment with nerve growth factor (NGF) causes sustained ERK activity and differentiation into neuron-like cells. Adding drugs that decrease or increase ERK signalling can convert the effect of NGF on ERK activity into an EGF-like effect, and vice versa. This perturbation causes an exchange in the outcome (EGF now drives



differentiation and NGF drives proliferation)<sup>60</sup>. Subsequent studies in which ERK-signalling dynamics were directly controlled with optogenetic inputs confirmed that differences in MAPK dynamics suffice to specify cellular differentiation in PC12 cells<sup>40,62</sup>. b | Using optogenetics, researchers showed that upstream signalling dynamics affect downstream pathways. In particular, signal transducer and activator of transcription 3 (STAT3) phosphorylation functioned as a persistent detector of ERK activation. In 3T3 fibroblast cells expressing an optically controllable son of sevenless homologue (SOS) construct (opto-SOS; an activator of the RAS GTPase), 2 hours of light stimulation caused a robust STAT3 phosphorylation. However, the same stimulus broken into two, 1-hour pulses did not cause STAT3 phosphorylation despite the activation of other ERK-responsive pathways<sup>40</sup>. Thus, optogenetic approaches have directly shown that cells respond to specific upstream signalling dynamics and have identified some of the pathways that respond to a particular signalling pattern. Part b reprinted from *Cell*, 155/1430, Toettcher, J. E., Weiner, O. D. & Lim, W. A., Using optogenetics to interrogate the dynamic control of signal transmission by the Ras/Erk module, 1422–1434, Copyright (2013), with permission from Elsevier.

The four photosensitive proteins that are at the core of current reversible optogenetic systems are compared (see the table). Note that some photosensitive proteins actually represent a collection of proteins from different organisms and have been used by different groups to control different signalling systems. This is particularly true of the light-oxygen-voltage (LOV) domains. This table summarizes the features for the entire classes of photosensitive proteins; the features will vary based on the particular protein used.

**Column heading definitions**

**Turn-on speed.** The speed with which the system activates when illuminated with stimulatory light ( $\lambda_{on}$ ).

**Turn-off speed.** The speed with which the system resets in the dark or when illuminated with inhibitory light ( $\lambda_{off}$ ).

**Chromophore requirement.** Lists the small molecule, if any, that is needed to make the protein photosensitive and whether it is naturally found in the cell or has to be provided.

**Compatible imaging wavelengths.** These wavelengths of light are not markedly stimulatory and can be used to image other fluorophores without notably activating the optogenetic system.

$\lambda_{on}$ . The wavelength (or wavelengths) of light that is most effective at activating the system. Wavelengths outside these ranges could still activate the system but may require higher intensities and/or longer exposures.

$\lambda_{off}$ . The wavelength, if any, that actively resets the system. Wavelengths outside this range could still inhibit the system but may require higher intensities and/or longer exposures.

**Effector affinity.** The order of magnitude approximation of the dissociation constant for a system. Heterodimerization affinities are listed for the systems that are based on PHYB-PIF<sup>18</sup> and the LOV-domain-based TULIP (tunable, light-controlled interacting protein) system<sup>15</sup>. The homodimerization affinity for Dronpa is listed<sup>19</sup>.

Photosensitive protein	Turn-on speed	Turn-off speed ( $t_{1/2}$ )	Chromophore requirement	Compatible imaging wavelengths (nm)	$\lambda_{on}$ (nm)	$\lambda_{off}$ (nm)	Effector affinity	Refs
PHYB	Seconds	• Seconds (illuminated at 750 nm) • Hours (dark reversion)	PCB; exogenous or synthesized <i>in situ</i>	≤514	650	750	• <100 nM (post 650 nm) • >100 μM (post 750 nm)	16–18
CRY2	Seconds	5 minutes	Flavin; endogenous	≥561	405–488	NA	Not determined	9–11
LOV	Seconds	Tens of seconds to minutes	Flavin; endogenous	≥514	440–473	NA	• 1 μM (dark) • 100 μM (light)	12–15, 67
Dronpa	Seconds	• Tens of seconds (illuminated at 390 nm) • Tens of minutes (dark reversion)	None	≥600	390	490	• 10 μM (post 490 nm) • >100 μM (post 390 nm)	19

CRY2, CRYPTOCHROME 2; NA, not applicable; PHYB, PHYTOCHROME B; PIF, PHYTOCHROME INTERACTING FACTOR.

**Box 1: Comparison of the reversible photosensitive proteins used in optogenetic systems**

## CHAPTER THREE: TECHNICAL PERFORMANCE AND TROUBLESHOOTING OF TWO OPTOGENETIC SYSTEMS

At the heart of this project is the light-regulated interaction of the T cell receptor (TCR) with a ligand on a supported lipid bilayer (SLB). Unlike most other cell-centric optogenetic experiments, the cell would not express all the required components. Instead, the cell would only express a receptor fused to the light-sensitive protein's binding partner. Therefore the light-sensitive protein would have to be purified and attached to the SLB separately. The following section details my efforts to use two different optogenetic systems to accomplish this goal.

I first tried using the PhytochromeB/PIF system<sup>1</sup>, but due to insurmountable technical issues, switched to a more facile LOV2 based system<sup>2</sup>. In short, the failure of the PhyB/PIF system was surprisingly not PhyB but PIF. In vitro, purified PhyB and PIF interacted robustly. However, once PIF was post-translationally conjugated to any sort of receptor, it lost all detectable binding to PhyB. Switching to the LOV2 based LOVTRAP system<sup>2</sup> proved to be one of the most fruitful decisions of grad school. The LOV2 expresses roughly 100 fold higher than PhyB in bacteria and the binding partner surface expresses and binds LOV2 when fused to a chimeric antigen receptor.

First, I'll detail my purification procedures and efforts to troubleshoot the PhyB/PIF interaction. Then I'll detail my more successful efforts with LOVTRAP.

As both PhyB and PIF needed technical troubleshooting, I'll detail them separately below.

### PhyB purification and troubleshooting

#### *Initial PhyB purification attempts from yeast*

My very first attempts to purify PhyB was of a longer truncation of PhyB (aa 1-917, plasmid DT71) from *S. cerevisiae*. No meaningful progress was made. Yields were very low and suffered from extensive proteolysis

of PhyB. I had initially taken this approach out of concern of the kinetics of PhyB switching between the Pr to Pfr forms. Biochemical studies of heterologously expressed PhyB in bacteria used the shorter 1-651aa truncation<sup>3</sup> never looked at the kinetics of PIF binding and unbinding. It wasn't until Anna Goldberg in the lab showed that PhyB 1-651 had indistinguishable PIF binding kinetics from PhyB 1-917 in NIH 3T3 cells that I decided to purify PhyB 1-651 from bacteria. So far as I can tell, there are no drawbacks to using PhyB 1-651 over PhyB 1-917.

### *Initial PhyB purification attempts from E. coli*

Plasmids from expression of PhyB (DT184, but DO NOT USE IT!) and PIF in E. coli were obtained from the Rosen lab<sup>3</sup>. Cells expressing PhyB also carried plasmids to express heme oxygenase (DT182) and phytochromobilin synthase (DT243; lacking the chloroplast transit peptide) in order to convert endogenous heme into phytochromobilin, the endogenous chromophore of PhyB.

PhyB was purified essentially as detailed in the final protocol detailed later, but without using a PIF-column. The resulting PhyB could photoreversibly interact with PIF-GFP, but had three problems:

1. PhyB immobilized onto Ni-NTA agarose beads recruited less and less PIF with each round of recruitment (Figure 5b).
2. The PhyB difference spectrum (simply the absorbance spectrum of Pr minus the absorbance spectrum of Pfr) decreased in amplitude after each round of photoconversion (Figure 5c).
3. PhyB "shredded" SLBs, tearing ~10-100 um sized holes in the bilayer. By contrast, mCherry-10xHis added to identical bilayers were fluid and uniform (Figure 5a).

These problems pointed to a problem with PhyB itself. By sheer luck, a visiting post-doc asked for one of the plasmids and prompted me to look back more closely at the PhyB coding sequence. It turned out that there was a four amino acid cloning scar (MGHM) on the N-terminus of this particular PhyB expression plasmid. Knowing that PhyB was generally intolerant of N-terminal fusions, I recloned the expression

plasmid to remove the four amino acids. This change completely solved all of the PhyB problems. PhyB could recruit Pif for dozens of photocycles (ie – transitioning from 650nm to 750nm light and back) without a measurable decrease in activity, the difference spectrum did not change over several photocycles, and bilayers functionalized with PhyB were fluid and uniform. All subsequent PhyB purifications were carried out with this construct (DT244) or similar derivatives.

Although the offending PhyB expression plasmid had been used in published work, I suspect the authors never noticed the decrease in activity because their experiments either held PhyB in the Pr or Pfr conformation. They never put PhyB through multiple photocycles and thus never would have seen the drop in activity.

## PIF purification and troubleshooting

Considering that PIF always expresses well and seems active in mammalian tissue culture cells while PhyB needs the most optimization, it was surprising that most troubleshooting for the purified proteins was focused on PIF. For clarity it is important to note that there are several PIFs (Phytochrome interacting proteins). Essentially all published work using PhyB in living cells uses PIF3 1-100aa<sup>1,4,5</sup>. For my in vitro system, I opted to use a fragment of PIF3 instead because it had already been successfully purified as an active protein<sup>3</sup> and we had unpublished data in the lab that PIF3 1-100aa recruited to PhyB in a similar manner as PIF6 1-100aa in living cells. Later, I purified GFP fusions to PIF1 1-100aa, PIF3 1-100aa and PIF6 1-100aa (the PIFs biochemically shown to interact with PhyB; DT202, DT203 and DT204) and tested their recruitment to PhyB in vitro. While all constructs photoreversibly bound PhyB, PIF3-GFP clearly had the best dynamic range (Figure 6). The other PIFs suffered from high basal binding. These data validate the choice of PIF3 as being the best PIF for in vitro work.

After identifying PIF3 as the best choice, I tried genetically fusing to the N-terminus of a chimeric antigen receptor. The receptor never made it to the surface and was not pursued further. Instead, I opted to post-translationally fuse purified PIF3 to a surface expressed CAR using the SpyCatcher system<sup>6</sup>. This approach had the additional advantage that it avoided any potential glycosylation or other post-translational modifications of PIF3 that might interfere with PhyB binding and could use protein that had already been validated to interact with PhyB.

For troubleshooting reasons, I had tried to purify PIF3 1-100aa with a unique cysteine for a PhyB binding assays using fluorescence anisotropy. This protein crashed out of solution after cleavage from the N-terminal SUMO3 tag. I tried to find slightly larger fragments of PIF3 that would be more stable. As PIF3 has no solved structure and essentially no predicted secondary structure, I used an online structured/unstructured program to try to find cut sites that would include more structured protein.

Based on this analysis, I chose cut sites after amino acid 132 and 151. PIF3 1-132aa remained soluble after proteolysis from SUMO3 and was used for any and all subsequent PIF3 purification.

Next, I purified a PIF3-SpyCatcher fusion (DT366). It reversibly bound PhyB and covalently conjugated to the CAR, as judged by surface localization as well as supershifting of the CAR by SDS-PAGE. Conjugation efficiency was substantially improved by incubating cells and PIF3-SpyCatcher in PBS pH 6.2 for 15 minutes (Figure 7). There was no obvious cell death or changes in morphology for this short incubation.

Despite effective conjugation and surface localization of PIF, there was no detectable interaction with PhyB. PhyB with a SNAP dye did not reversibly translocate to the cell surface, despite their being substantial levels of dye-conjugated PIF-SpyCatcher on the surface. Additionally, PIF-functionalized cells did not spread on SLBs coated with PhyB, as would be expected when cells activate. There wasn't even a small cell footprint, which one would expect if there was only a physical PhyB-PIF interaction that did not cause cell activation.

Despite no obvious PhyB/PIF interaction, I tried to see if perhaps an undetectable PhyB/PIF interaction was causing cell signaling. In analogy to the well-established pMHC tetramers, I made PhyB tetramers by purifying biotinylated PhyB and tetramerized it using streptavidin. Tetramers were purified from monomers by gel filtration and confirmed on a native polyacrylamide gel. Tetramers were incubated with PIF-functionalized Jurkats in red or infra-red light for 5 minutes at 37C and assayed for Erk phosphorylation by flow cytometry. In short, I never observed any PhyB dependent Erk phosphorylation under any condition. The CAR was capable of signaling, as stimulation with the OKT8 antibody induced robust Erk phosphorylation comparable to that produced through the native TCR complex with the OKT3 antibody. Additionally, the PhyB tetramers never stained the cells above background, suggesting a total absence of a PhyB-PIF interaction.

Because the PhyB used to make the tetramers was purified with a PIF column, it seemed unlikely there was a problem with PhyB's specific activity or the tetramer's ability to cluster the CAR. But the failures so far could be explained if only a small fraction of PIF molecules were able to bind PhyB. A low specific activity of PIF would not have been obvious in recruitment assays when PIF was in vast excess of PhyB. To more directly measure the fraction of functional PIF molecules, I performed a native gel shift assay. Whether adding monomeric or tetramerized PhyB in excess, it consistently showed about 72% of the PIF supershifted, indicating the vast majority of PIF molecules could bind PhyB in vitro (Figure 8). Note that 72% is a lower bound on the fraction of active PIF molecules. Some PhyB-PIF complexes could dissociate as the gel runs (though the gel was kept in the dark while being illuminated from the side with red light) and higher concentrations of PhyB could supershift more of the PIF. In all, the evidence suggests that the vast majority of both PhyB and PIF molecules remain active after purification and cannot account for the lack of a PhyB-PIF interaction or lack of signaling.

It could be possible that the cells or something in the media was killing PhyB or PIF activity or otherwise interfering with the interaction. Although most signaling and microscopy experiments were done in PBS, I pushed the system to test the durability of the PhyB/PIF binding activity. Ni-NTA agarose beads functionalized with PhyB were added to wt Jurkat cells in complete growth media along with soluble PIF3-GFP. PhyB still effectively recruited PIF under these conditions. Next, the mixture of cells, PhyB and PIF incubated overnight at 37C in a tissue culture incubator. The next day, PhyB still recruited significant amounts of PIF3-GFP, albeit noticeably lower amounts than before. However, cultures that contained 0.5 mM BME during the overnight incubation retained most (but not all) of the original activity (Figure 9). Therefore it seems as if the PhyB-PIF interaction is very robust, so long as PIF is not conjugated to a CAR. I found no evidence of any media components or soluble factors from the cells that impede the PhyB-PIF interaction.



It seemed as if somehow PIF lost all activity once it was conjugated to the CAR. In a last ditch effort, I did a small screen of all PIF, receptor and PhyB variants I could think of to stimulate the cells (Figure 10). For PIF, I functionalized receptors with both monomers and dimers of PIF. For the CAR, I tried reversing the placement of the SpyTag and SpyCatcher domain. I even tagged CD3e of the TCR complex with SpyCatcher, in the hopes that the native receptor would be more sensitive than the CAR. For PhyB, I tried stimulating both with tetramers and Ni-NTA agarose beads coated with PhyB. None of these permutations showed any hint of signaling, as assayed by Erk phosphorylation with flow cytometry. The most important positive control was to functionalize receptors with a PIF that still retained a 10xHis tag from purification. When these cells were incubated with plain Ni-NTA agarose beads, they produced robust signaling. These data indicate that if bound, PIF-functionalized receptors induce robust signaling. I concluded that for unknown reasons, PhyB could no longer bind PIF once it had been conjugated to a receptor.

In all, for unknown reasons it appears that while PIF robustly binds PhyB in vitro, it loses all detectable activity once it conjugates to a receptor on the cell surface. I doubt the SpyCatcher-SpyTag chemistry interfered in any way, as PIF3-SpyCatcher conjugated to SpyTag-GFP still reversibly bound PhyB on a Ni-NTA agarose bead. I believe that PIF3 partially denatures on the cell surface or its conformation is otherwise altered so that it can no longer bind PhyB. I think this is a consequence of PIF3 (or any other PhyB binding domain of a PIF) having little to no secondary structure. An engineered PhyB binding partner with more structure would likely have retained its shape and activity and would have made these experiments possible. As described below, such an engineered binding partner to LOV2 behaved beautifully.

Having thoroughly exhausted every chance to fix the PhyB-PIF interaction, I switched to another optogenetic system, one based on the interaction between LOV2 and an engineering binding partner.

## The LOVTRAP system

### *Introduction: Why choose the LOVTRAP system?*

Because of the failure of PhyB to interact with PIF once PIF was conjugated to a cell surface receptor, I considered alternative optogenetic systems. While there are many to choose from, binding between the two proteins is usually induced by light and then reverts in the dark. However, a major goal in developing a light-gated T cell receptor was to make a tool to test the kinetic proofreading model. Since the model predicts that longer receptor-ligand interactions are more likely to trigger a receptor, I sought to directly manipulate the ligand off-rate with light. With the PhyB/PIF system, infrared light directly dissociated the pair. However, most alternative systems bind upon illumination and unbind in the dark. Light does not change the off-rate.

Besides the PhyB/PIF system, there were two systems with light-induced dissociation. The first is based on the photoactivatable protein Dronpa<sup>7</sup>. In short, it takes advantage of small conformational changes in Dronpa when it is photoactivated to regulate its binding to another (dark) Dronpa protein. The drawback of the system is that dissociation kinetics were slow relative to the normal T cell receptor-ligand interactions. Dronpa dissociates on the tens of seconds to minute timescale while receptor ligand interactions are usually in the range of seconds to hundreds of milliseconds.

The second system with light-induced dissociation is the LOVTRAP system<sup>2</sup>. The blue-light sensitive protein is the LOV2 photosensory domain of phototropin1 of *Avena Sativa*. Its binding partner, Zdk, is an engineered protein, a small three alpha helix bundle derived from the Z domain of the staphylococcal protein A. Uniquely, Zdk was selected to bind LOV2 dark state conformation with much higher affinity than the lit state conformation. Thus exciting LOV2 with blue light causes Zdk to dissociate, exactly what is needed to test the kinetic proofreading model. Fortunately, experiments in cells showed that Zdk releases from LOV2 on the order of seconds, fast enough to test the kinetic proofreading model.

The following sections will detail my efforts to purify LOV2 and Zdk, and the troubleshooting needed to use it as a robust tool to interrogate T cell receptor signaling.

### *Measuring Zdk-LOV2 dissociation kinetics and titrating it with light*

Before I could use the LOVTRAP system to test kinetic proofreading, I had to verify that titrating the intensity of blue light could indeed titrate the LOV2-Zdk off-rate. Additionally, I wanted to know that at higher intensity, saturating blue light, that the two proteins dissociated sufficiently fast from one another that I could mimic endogenous ligand dissociation kinetics. If the receptor does use kinetic proofreading, I would be most likely to observe it by enforcing ligand dissociation kinetics similar to wild type ligands.

Because I wanted to ultimately measure signaling of T cells on a supported lipid bilayer, I measured the Zdk dissociation kinetics from LOV2 attached to a bilayer. Saturating amounts of purified LOV2 (DT481) was added to a supported lipid bilayer, attaching via its 10xHis tag and the Ni-NTA lipid head groups. Cy3 labeled Zdk (DT482) was added to a final concentration of 250 nM in dPBS, roughly 10 times the published  $K_d$  of the interaction in the dark. Zdk bound to LOV2 on the SLB was measured using TIRF as they were acutely illuminated with different intensities of blue light (470nm). The loss of fluorescence was fit to a single exponential decay and the corresponding apparent rate constant recorded. This procedure was repeated, sampling the entire range of the blue LED. The results are shown in Figure 11. By titrating the intensity of blue light, I could enforce Zdk-LOV2 binding half-lives as short as 700ms.

I never put much effort to determine the half-life of the interaction while kept in the dark. Zdk must dissociate from the dark-state conformation of LOV2 at some slow rate, which represents the maximum half-life I could enforce with the system. While I never did it empirically, I suspect the dissociation half-life in the dark is on the order of minutes. Fitting the apparent dissociation rate constant to LED intensity did not benefit from including a term allowing for Zdk-LOV2 dissociation in the dark. Thus over the range of

LED intensities I used, the dominant factor controlling the half-life of the Zdk-LOV2 interaction is the intensity of blue light.

For anyone reading this and considering measuring the dark-state dissociation rate, it must be done by washing in a large pool of unlabeled Zdk. FRAP will likely also damage the LOV2 protein, interfering with the recovery after photobleaching.

Plotting the apparent rate constant as a function of LED intensity showed evidence of saturation at higher LED intensities. Observing saturation was reassuring, as it indicated the blue LED was bright enough to push the system close to its fastest off-rate. We could not make the system go faster by shining more light on it. The data were fit by using a two-step dissociation model. In the first step, blue light induces a change in LOV2, but it still remains bound to Zdk. The rate of the reaction is linearly proportional to the intensity of blue light. In a second step, Zdk dissociates from the lit state of LOV2 in a light-independent manner. Values for the two rate constants were determined using non-linear regression. The data were extremely well fit by the model. This model was used in subsequent experiments to infer the Zdk-LOV2 dissociation rate at a given LED intensity. As stated above, adding a term to allow Zdk dissociation directly from the dark state of LOV2 did not noticeably improve the model.

### *Making a Zdk-chimeric antigen receptor*

Knowing that the Zdk-LOV2 interaction was fast and titratable, I next needed to know if LOV2 still interacted with Zdk when Zdk was part of a chimeric antigen receptor. Initially, I planned to post-translationally conjugating Zdk to a chimeric antigen receptor using SpyCatcher, as I had done with PIF. However, I sometimes observed that merely the act of conjugating Zdk to the CAR could induce signaling. So I went back to the simple approach of genetically fusing Zdk to the N-terminus of the CAR. By luck and good fortune, this Zdk-CAR (DT484) both trafficked to the surface and interacted with LOV2. Dye-labeled

soluble LOV2 localized to the surface of CAR-expressing cells and reversibly dissociated with blue light. Similar to the activity on bilayers, LOV2 association with the CAR was titratable with blue light (Figure 12). That Zdk trafficked to the surface and remained functional is a testament to the robustness of Zdk and binding partners engineered from a similar backbone. Similar CARs fused to the SspB (the LOV2 binding partner in the iLID system<sup>8</sup>) trafficked to the surface but could not bind their corresponding LOV2 variant. I think the small, well-structured nature of Zdk is the reason the LOVTRAP system succeeded where the PhyB/PIF system failed. The unstructured nature of PIF means that its shape and therefore activity are more sensitive to the surrounding environment. By contrast, the three alpha-helix bundle of Zdk allows it to remain well-structured and its small size makes it a good fusion partner. If an analogous binding partner for PhyB could be engineered, it would greatly improve the system, both in vivo and in vitro.

#### *The LOV2:Zdk-CAR interaction photoreversibly activates the T cell signaling pathway*

With a confirmed LOV2:Zdk-CAR interaction, I wanted to see if it was sufficient to activate signaling in cells. Jurkat cells expressing the CAR and a diacylglycerol (DAG) live cell reporter (DT326) were dropped onto supported lipid bilayers functionalized with LOV2. From previous experience, I felt the DAG reporter was the easiest to use and had a large dynamic range. Cells were alternatively illuminated with two minutes of maximum intensity blue light or no blue light. Amazingly, there was a clear, unambiguous recruitment of the DAG reporter to the plasma membrane that anti-correlated with the presence of blue light. (Blue light should terminate the LOV-CAR interaction and thus terminate signaling.) Qualitatively similar results were seen with fluorescently tagged ZAP70 and Grb2 (DT328 and DT327, respectively).

Unfortunately when I pressed the system towards longer time courses with oscillating blue light, I consistently observed that cells became less and less responsive over time. After 15 or so on the scope, cells would typically withdraw to a very small footprint and neither spread nor signal when kept in the

dark. Frustratingly, I also observed a loss of Zdk recruitment to LOV2 on a bilayer, in a completely in vitro setting. Somehow over time LOV2 was losing activity.

### *Successfully troubleshooting the loss of LOV2 activity*

I won't detail all of the troubleshooting I did with the system, only the two changes that I believe are necessary so that LOV2 retains full activity over time.

First, the method of LOV2 attachment to the bilayer matters. When tracking LOV2 activity (specifically, its ability to recruit Zdk) on bilayers in vitro, I noticed that not only did the region I was imaging lose activity over time, but regions far from where I imaged also had reduced activity. This suggested a light-independent mechanism for the loss of activity. Curiously, the total amount of dye-labeled LOV2 on the bilayers seemed to decrease substantially over time. The LOV2 carried a 10xHis tag (a standard attachment method for proteins to Ni-NTA containing bilayers) yet the concentration of a 10xHis-GFP on the bilayer did not change over time. Though I never bothered with the detailed experiments to prove it, I believe LOV2-10xHis leaches off the Ni-NTA bilayers on the order of minutes to tens of minutes, resulting in a loss of activity, both in vitro and with cells.

Fortunately, the loss of LOV2 from the bilayers is completely stopped by using the biotin-streptavidin interaction to attach the protein. Biotinylated LOV2 (with the 10xHis tag proteolytically removed; DT493 or its derivatives, DT494 and DT495) are attached to bilayer contained a lipid with a biotinylated head group via a streptavidin intermediate. Attached in this way, the LOV2 concentration on the bilayer remains constant over time.

Unfortunately, despite being able to keep the amount of LOV2 on the bilayer constant over time, I still observed a significant decrease in LOV2 activity after each round of Zdk recruitment and release. However, the decrease in activity was restricted only to the area I was imaging, suggesting that the prolonged blue light exposure could be bleaching the flavin chromophore. Using a commercial oxygen

scavenging system (ProLong Live Antifade Reagent, ThermoFisher Scientific) prevents nearly all of the loss of LOV2 activity. Importantly though, the buffer needs to be treated with the reagent for at least 90 minutes at room temperature to effectively scavenge the oxygen. Adding the antifade reagent just prior to imaging has no effect.

Combining both a biotin-based method of attachment and an oxygen scavenging system allows the LOV2 to retain activity over many cycles of recruitment, both completely in vitro and with cells. In the most strenuous test, Jurkat cells expressing the Zdk-CAR and Zap70-mCherry had no apparent loss in activity even after over three hours of imaging (Figure 13). As nearly all the imaging time courses are 45 minutes or less, it is safe to say there is negligible change in LOV2 activity over that time.

Although much time was spent trying to get the PhyB/PIF system to induce T cell signaling, in the end unknown and insurmountable technical barriers prevent its use. Fortunately, the LOVTRAP system proved to be a competent substitute. Despite two unanticipated troubleshootings, the system now works consistently to recruit Zdk in vitro and stimulate T cell signaling in vitro. The following sections will detail my efforts to use the optimized system to answer biological questions in T cell signaling.

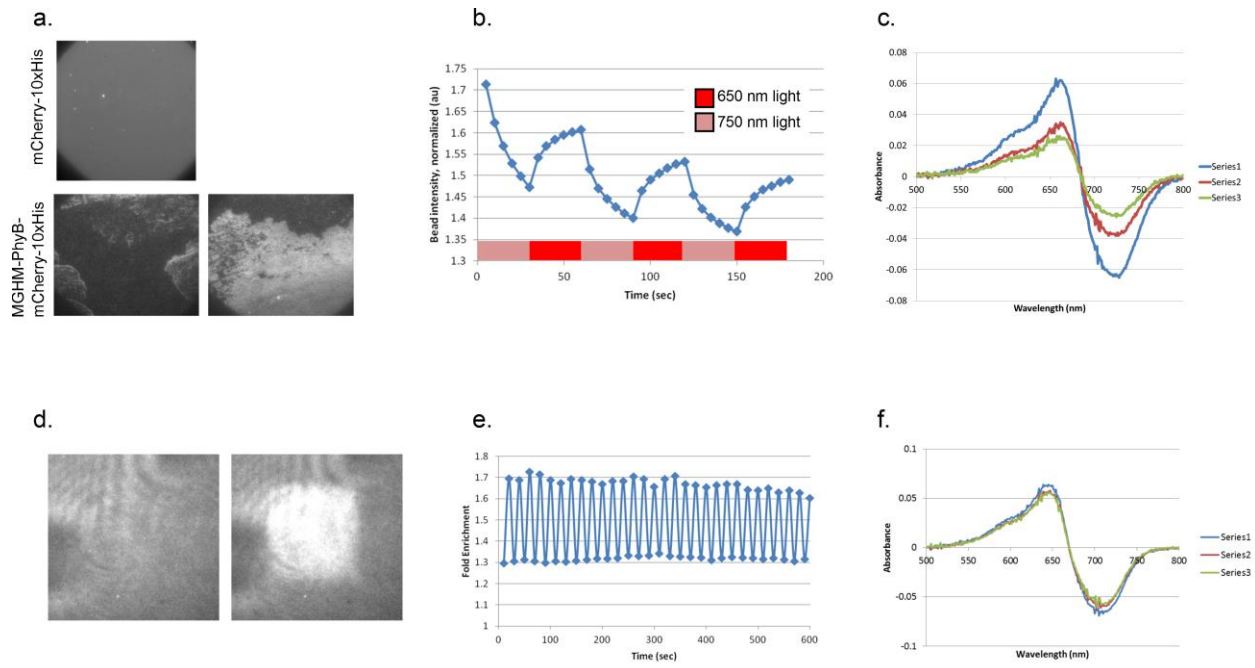


Figure 5: Comparing functionality of PhyB with and without four extra N-terminal amino acids

a) MGHM-PhyB added to supported lipid bilayers results in large scale destruction. By contrast, mCherry-10xHis added to identically prepared bilayers is largely uniform and fluid (FRAP data not shown). Imaged in TIRF.

b) Ni-NTA agarose beads were loaded with MGHM-PhyB and recruited Pif-GFP, cycling several times between red and infra-red light. Each round of recruitment shows a significant reduction in activity.

c) Reduced activity is PhyB intrinsic. The three difference spectra of MGHM-PhyB (the absorbance spectra of Pr minus the absorbance spectra of Pfr) were taken one after another. The reduced intensity indicates reduced amounts of a light-absorbing PhyB species.

d) Wild type PhyB, lacking the four MGHM N-terminal amino acids, can spatially recruit Pif-GFP onto supported lipid bilayers. Red light was projected in the square, infra-red light was project outside the square. Pif-GFP recruitment was imaged in TIRF. Bilayers remained fluid and uniform with the wt PhyB.



e) Pif-GFP recruitment over dozens of photocycles was measured. There is a negligible drop off in activity over the time course.

f) The wt PhyB difference spectra shows no reduction in intensity over three photocycles.

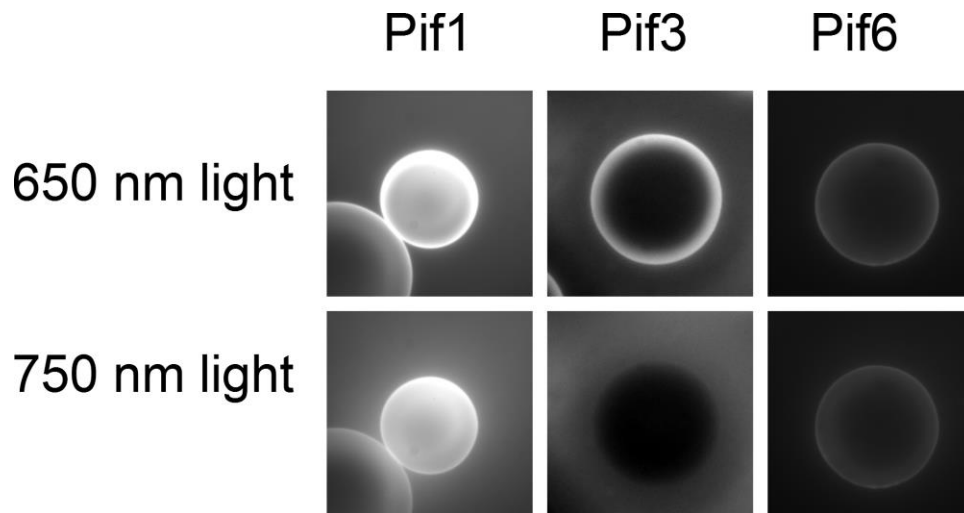


Figure 6: Pif3 has the largest dynamic range binding to PhyB of Pif1, Pif3 and Pif6

The indicated Pif-GFP fusions were purified (DT202, DT256 and DT204 for Pif1, Pif3 and Pif6, respectively) and reversibly recruited to Ni-NTA agarose beads functionalized with PhyB-10xHis. All Pif concentrations were normalized to 1 $\mu$ M. The brightness and contrast of each pair of Pif images was adjusted to try and show the largest dynamic range in recruitment.

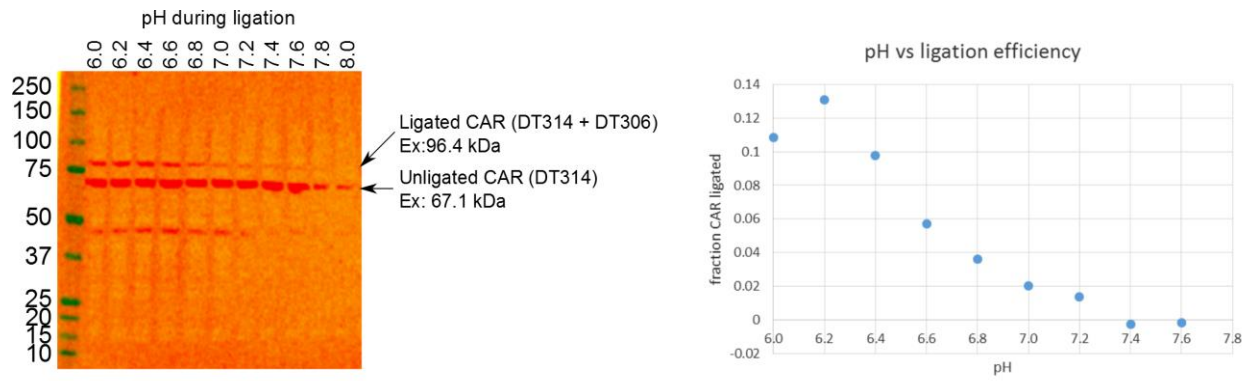


Figure 7: A lower pH promotes SpyCatcher ligation

(Left) Anti-HA western blot showing the supershifting of CAR DT314 upon ligation with SpyCatcher-Pif (DT306). Ligations were carried out at room temperature for 15 minutes, in dPBS adjusted to the indicated pH. (Right) The fraction of ligated CARs was quantified by densitometry from the western blot and plotted as a function of ligation pH.

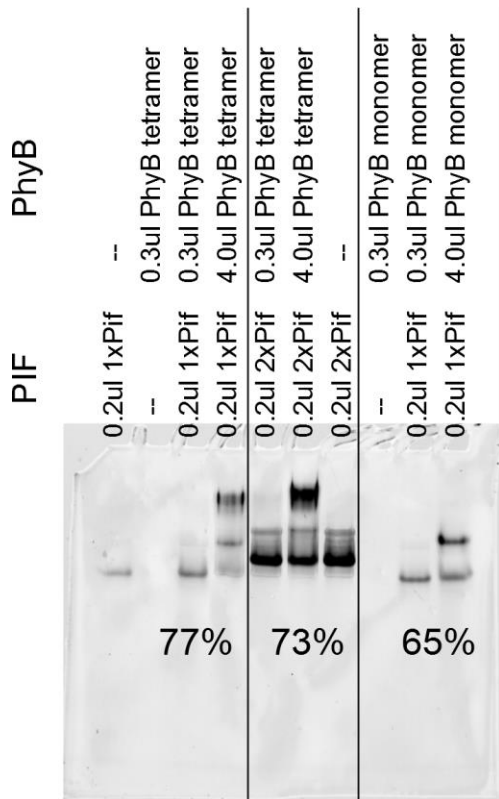


Figure 8: The majority of Pif molecules are active and capable of binding PhyB

Native gel shift assay, showing the majority of Pif molecules, whether a monomer or tandem dimer, supershift in the presence of PhyB monomers or tetramers. PhyB is unlabeled and Pif is labeled with fluorescein. Numbers indicate the percentage of Pif molecules that super-shifted for conditions with 4.0ul PhyB. Gel imaged on a Typhoon scanner, 488nm laser as the excitation source and a 526 short pass filter. The concentrations of PhyB and Pif are not recorded, but sufficient PhyB can be added to supershift the majority of Pif molecules. Gel was run in the dark, except being constantly illuminated with light from a red LED.

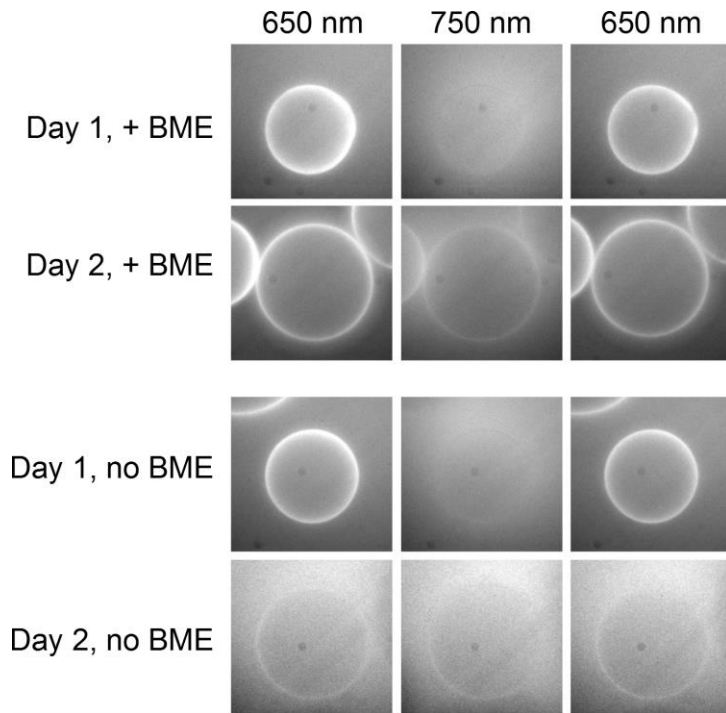


Figure 9: PhyB retains significant activity after overnight incubation with cells

Ni-NTA agarose beads were loaded with PhyB-10xHis and added to Jurkat cells growing in complete media (RPIMI 1640 +10% FBS, +2mM L-glutamine). 0.5 mM BME was added as indicated. PhyB activity was assayed by adding beads to 1  $\mu$ M Pif3-GFP in dPBS and reversibly recruiting with alternative 650 nm and 750 nm light, imaged by confocal microscopy. PhyB activity was assayed either immediately after adding to the cells in growth media (Day 1) or after overnight incubation in a tissue culture incubator at 37C and 5% CO<sub>2</sub>. Without BME, PhyB showed small, but measurable activity after overnight incubation. However with BME, PhyB retained most of its activity, with a slight increase in basal Pif3-GFP binding. While it is not surprising that a reducing agent helped preserve much of PhyB's activity, the experiment shows that nothing in the complete growth media nor any substance secreted by the cells inhibited PhyB activity. Thus it is very likely that PhyB remains active when mixed with cells during signaling assays.

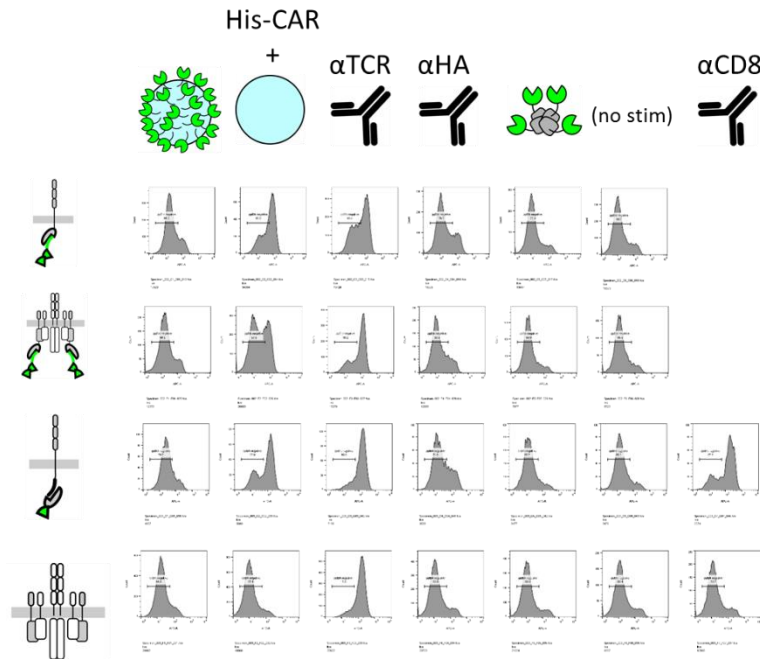


Figure 10: PhyB cannot induce signaling when Pif is conjugated to a cell-surface receptor

Cell lines are cartooned on the left column and treatments are cartooned on the top row. The cell lines from top to bottom are: SpyCatcher-CAR (DT441) conjugated to a Pif tandem dimer, CD3e Jurkat knockouts expressing SpyCatcher-CD3e (DT436) conjugated to a Pif tandem dimer, SpyTag-CD8-CAR (DT314) conjugated to a monomeric Pif and wt Jurkats (containing only the wt TCR). Cell lines are polyclonal but stably express the receptors after lentiviral infection. Treatments from left to right are: Ni-NTA agarose beads functionalized with PhyB-10xHis, plain Ni-NTA agarose beads with the cell receptors being functionalized with Pif still containing a 10xHis tag, mAb OKT3 (1 ug/ml), anti-HA antibody (1 ug/ml), PhyB tetramers, no stimulation and mAb OKT8 (for anti-CD8 based CARS). Cells were stimulated for 5 minutes as indicated. Histograms are of the resulting ppErk staining by flow cytometry.

All cell lines showed minimal ppErk when unstimulated. Importantly, all the receptors induced robust ppErk when functionalized with a Pif-10xHis and exposed to plain Ni-NTA agarose beads, showing binding to the functionalized receptors is sufficient to induce signaling. Moreover, OKT3 stimulation showed all cell lines were capable of signaling. Unfortunately, PhyB either presented on a Ni-NTA bead or as

tetramers failed to induce ppErk above the unstimulated condition. This experiment convinced me to stop using PhyB/Pif and move on to another optogenetic system.

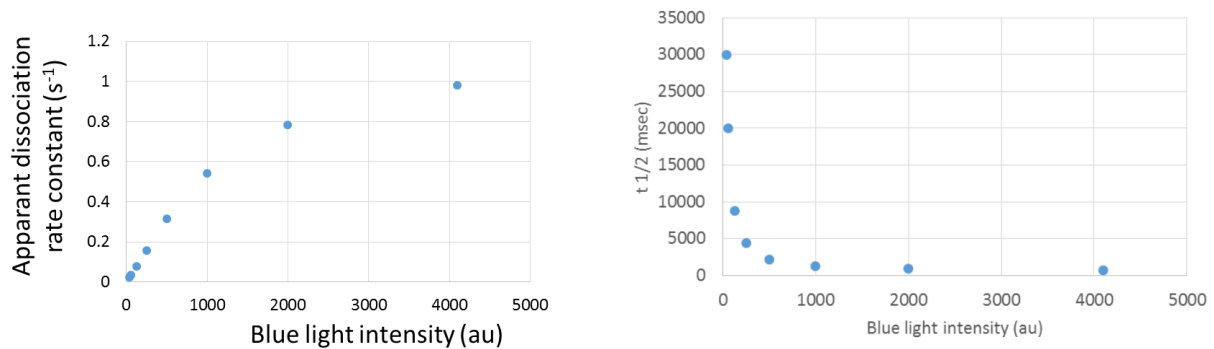


Figure 11: Titrating blue light intensity titrates the Zdk binding half-life

Supported lipid bilayers were functionalized with wt LOV2 and 250nM Zdk-Cy3 was added in dPBS. The apparent dissociation rate of Zdk from the bilayer was measured after acute illuminate with blue light (470 nm). Photobleaching was minimal, as persistent imaging with the 561nm laser produced no significant bleaching on the timescale of imaging, and was ignored. Zdk dissociation was well fit by a single exponential decay and the dissociation rate was calculated from a nonlinear regression. The same data is plotted in both graphs. When the apparent dissociation rate constant is plotted, there is a clear linear relationship between blue light intensity and dissociate rate constant at low light intensity, which begins to saturate at higher light intensities. Plotting the half-life of dissociation (right) provides a most intuitive sense of the timescales enforced with by changing the intensity of blue light. Blue light intensity refers to the 12 bit LED control (0-4095), as controlled with custom MATLAB code and a digital-to-analogue converter. A value of 4095 corresponds to 5V applied to the LED.



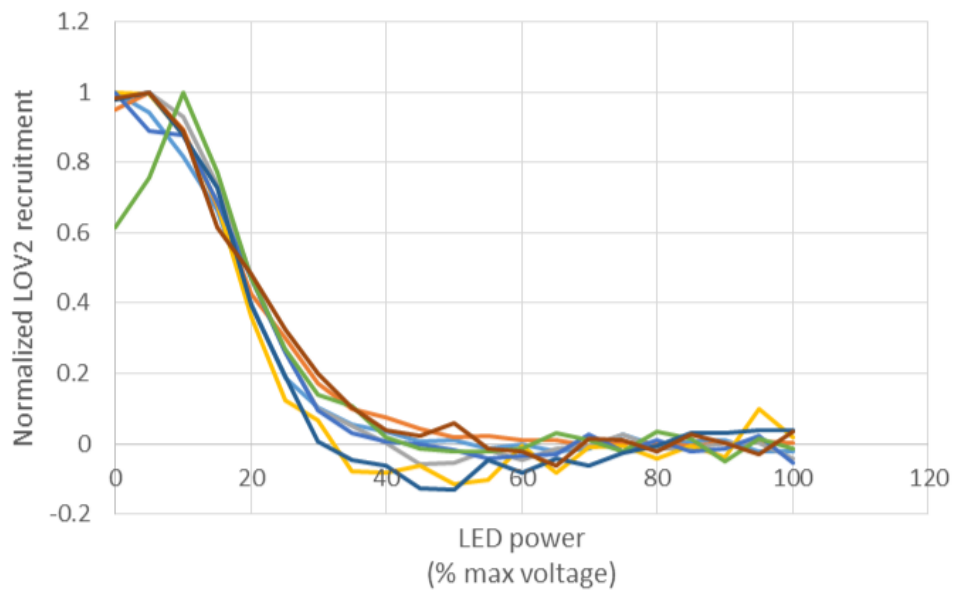
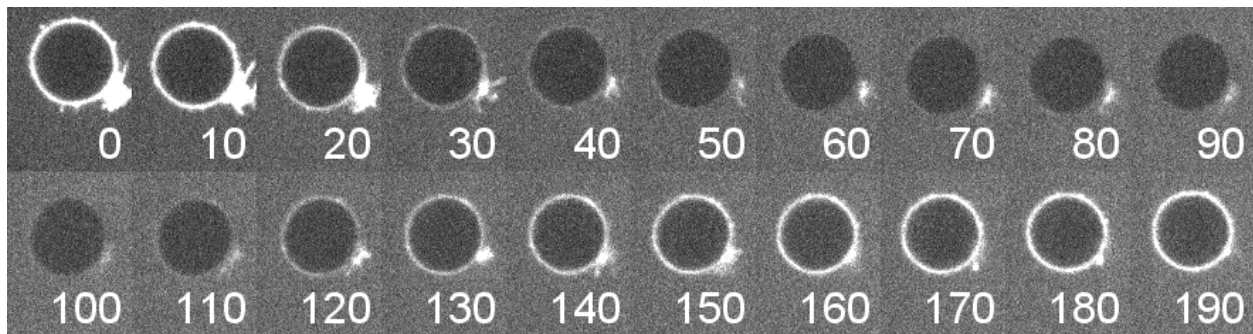


Figure 12: LOV2 recruitment to a Zdk-CAR is reversible and titratable

Jurkats stably expressing a Zdk-CAR (DT484) were added to dPBS with 250nM LOV2 labeled with a red SNAP dye (DT481). LOV2 recruitment to the cell surface was imaged with confocal microscopy. (Top) Montage of LOV2 recruitment as the blue LED slowly increases in power for the first 100 seconds. After 100 seconds, the blue light is turned off and LOV2 binding recovers. Numbers indicate time in seconds. (Bottom) LOV2 recruitment to multiple cells was quantified as a function of LED power. Max voltage is 5V. LOV2 dissociates much more rapidly with acute illumination with strong blue light, indicating LOV2 binding was measured at near equilibrium.

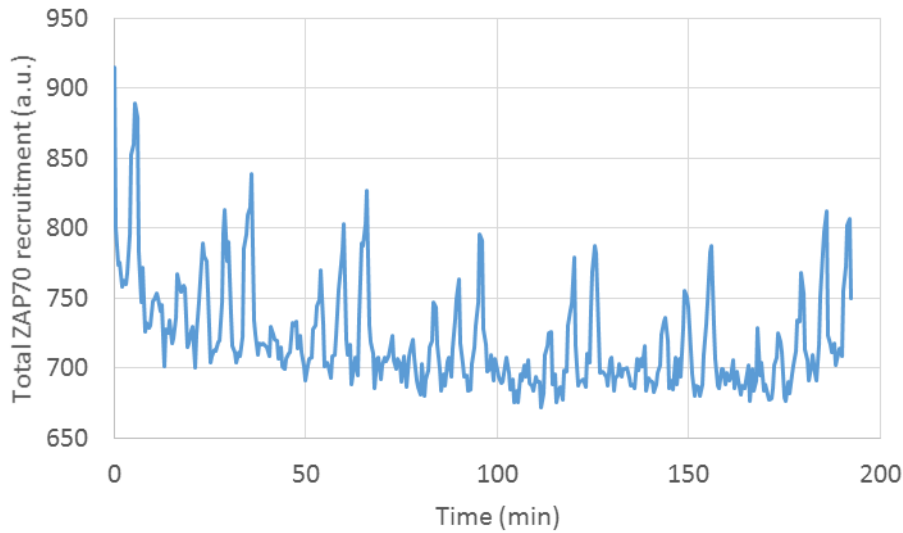


Figure 13: LOV2 remains active for hours

Supported lipid bilayers were functionalized with LOV2 V529N (DT552) via the biotin-streptavidin method. Jurkat cells expressing both the Zdk-CAR (DT484) and the ZAP70-mCherry reporter (DT523, clone B2) were added in dPBS +0.5 mM BME, 1 mg/ml beta casein that had been pretreated for at least 90 minutes with the oxygen scavenger. Cells were illuminated with alternating intensities of blue light that decreased in intensity over ~40 minutes, repeated for 6 cycles. ZAP70 recruitment was measured with a 561nm laser with TIRM. Total ZAP70 recruitment, not normalized for cell area, is plotted. The data shows that cells remain responsive to LOV2 stimulation for over 3 hours. Without the oxygen scavenger pretreatment, cells are rarely responsive beyond 15 minutes.

## References

1. Levskaya, A., Weiner, O. D., Lim, W. A. & Voigt, C. A. Spatiotemporal control of cell signalling using a light-switchable protein interaction. *Nature* **461**, 997–1001 (2009).
2. Wang, H. *et al.* LOVTRAP : an optogenetic system for photoinduced protein dissociation. (2016). doi:10.1038/nmeth.3926
3. Leung, D. W., Otomo, C., Chory, J. & Rosen, M. K. Genetically encoded photoswitching of actin assembly through the Cdc42-WASP-Arp2/3 complex pathway. *Proc. Natl. Acad. Sci. U. S. A.* **105**, 12797–802 (2008).
4. Toettcher, J. E., Gong, D., Lim, W. a & Weiner, O. D. Light-based feedback for controlling intracellular signaling dynamics. *Nat. Methods* **8**, 837–9 (2011).
5. Toettcher, J. E., Weiner, O. D. & Lim, W. a. Using optogenetics to interrogate the dynamic control of signal transmission by the Ras/Erk module. *Cell* **155**, 1422–34 (2013).
6. Zakeri, B. *et al.* PNAS Plus: Peptide tag forming a rapid covalent bond to a protein, through engineering a bacterial adhesin. *Proceedings of the National Academy of Sciences* **109**, E690–E697 (2012).
7. Zhou, X. X., Chung, H. K., Lam, A. J. & Lin, M. Z. Optical control of protein activity by fluorescent protein domains. *Science* **338**, 810–4 (2012).
8. Guntas, G. *et al.* Engineering an improved light-induced dimer (iLID) for controlling the localization and activity of signaling proteins. *Proc. Natl. Acad. Sci. U. S. A.* **112**, 112–7 (2015).

## CHAPTER FOUR: TESTING THE KINETIC PROOFREADING MODEL

To directly test the kinetic proofreading model, one needs to enforce a desired ligand-receptor dwell time and observe the magnitude of downstream signaling. To accomplish this, I constructed a clonal Jurkat cell line that expressed three proteins: a Zdk-CAR (DT484), Zap70-mCherry (DT523) and the extracellular and transmembrane domain of CD148, tagged N-terminally with a 10xHis tag (DT 502). This cell line is extremely robust, showing little drift in expression over several months in culture. During experiments, most every cell spreads and reversibly recruits Zap70-mCherry to the plasma membrane. It was very important to use fluorescence activated cell sorting (FACS) to select for single cell founders with low expression of Zap70-mCherry, expressed roughly at a 1:1 ratio with endogenous Zap70. If not sorted, polyclonal Jurkats expressing Zap70-mCherry after lentiviral infection express Zap70-mCherry roughly 10 fold above endogenous Zap70. As a result, the reporter persistently localizes to the plasma membrane, with no observable reversible recruitment in response to light. The addition of 10xHis-CD148 (EX and TM) helps the cells to passively adhere to the SLB, which contains 2% Ni-NTA lipids, but is otherwise not functionalized with His-tagged proteins.

Cells from this clonal line were added to SLBs functionalized with different concentrations of LOV2 V529N-Alexa488. To enforce different ligand dwell times, LOV2 was exposed to different intensities of blue light. Each intensity of blue light was held for three minutes, long enough for the cells to reach steady state where there was little change in translocated Zap70-mCherry. Cells were exposed to 10 different blue light intensities in this manner, spanning the range from minimal to maximal Zap70-mCherry translocation and alternated high and low intensity light to minimize any history dependent effects on signaling. At the end of each three minute segment, both the amount of translocated Zap70-mCherry and the amount of LOV2 enriched under the cell were measured (Figure 14).

Plotting the receptor occupancy (the amount of LOV2 under the cell) versus Zap70-mCherry recruitment showed a strikingly linear relationship over the entire range of receptor occupancy (Figure 14). Even with fine sampling at lower receptor occupancy, there does not appear to be any threshold receptor occupancy needed before Zap70-mCherry recruitment.

It is notable that the relationship between receptor occupancy and Zap70-mCherry recruitment is so linear, despite the data points being acquired “out of order.” Blue light was varied alternating between high and low intensities, which exposed the cell to alternatively low and high receptor occupancy. That the data points ended up forming such a straight line strongly suggests that Zap70-mCherry recruitment to the CAR is history independent.

The core kinetic proofreading model<sup>1</sup> predicts that:

$$\log(S/S_0) = n \cdot \log(\tau/\tau_0) \quad (1)$$

where  $S$  is the magnitude of signaling with a ligand binding half-life  $\tau$ ,  $S_0$  is the magnitude of signaling with a ligand half-life of  $\tau_0$  and  $n$  is the number of proofreading steps.  $S_0$  and  $\tau_0$  are a reference condition (the choice is arbitrary) to which all other half-life/signaling pairs are compared. Plotting  $\log(S/S_0)$  as a function of  $\log(\tau/\tau_0)$  (a “log-log” plot), yields a line whose slope is equal to  $n$ .

A log-log plot using either membrane-recruited Zap70-mCherry or CAR occupancy as the “signal” gives a slope of roughly one across a 10 fold range in LOV2 concentration (Figure 15 **Error! Reference source not found.**). A slope of one indicates no kinetic proofreading. It is simply the first “step” of a ligand binding its receptor. This can be seen from equation 1. Setting  $n := 1$ , the equation simplified to

$$S/S_0 = \tau/\tau_0 \quad (2)$$

Doubling the ligand lifetime (which doubles receptor occupancy) also doubles the signaling output, as would be expected for a system at thermodynamic equilibrium.

That treating CAR occupancy as the “signal” shows a slope of roughly one serves as a positive control for the experiment. We expect a ligand to bind its receptor in equilibrium. This observation is an independent way of verifying that light actually changes the ligand binding half-life and that part of the signaling pathway behaves in an expected manner.

Significantly, a log-log plot using Zap70-mCherry membrane recruitment as the “signal” shows largely the same trend, having a slope of roughly one. What’s more, the Zap70-mCherry curve nearly overlays the CAR occupancy curve, strongly indicating that there are no proofreading steps between ligand binding and Zap70 recruitment. Zap70 recruitment is simply proportional to the number of occupied CARs.

Is kinetic proofreading wrong? As always, more experiments are needed. Certainly the data indicate there is no effect of ligand binding half-life up through the point of Zap70 recruitment. This implies that searching for an active molecule of Lck and subsequent ITAM phosphorylation is not kinetically driven. However, other steps must occur before the receptor can signal to downstream components. Phosphorylation of the activation loop as well as tyrosines in interdomain B help to fully activate the kinase and relieve autoinhibition<sup>2-6</sup>, and could be steps in a kinetic proofreading pathway. The Zap70-mCherry reporter does not report on these activities.

Using reporters of more downstream signaling steps would help answer these questions. Reporters for Lat phosphorylation, the direct target of Zap70, would effectively capture any kinetically driven steps in Zap70’s phosphorylation and activation. Such reporters include fluorescently tagged Grb2 or Slp76. Assaying further down the pathway is less useful, as the further the signal gets from the receptor, the harder it is to answer the question of how the *receptor* discriminates ligands. Perhaps the T cell is able to sense the half-life of a ligand further down the cascade, but it seems the activity would not be part of the receptor itself. Knowing the properties of a signaling pathway and where they emerge is important when trying to understand the mechanism. Much effort is spent trying to understand mechanistically how the

proteins of the TCR discriminate ligands, from studying catch-bond formation<sup>7</sup>, to ITAM protection<sup>8-10</sup>, to tension sensing<sup>11,12</sup>. But these all assume the receptor itself discriminates between ligands. If that activity rested elsewhere in the pathway, it would be very valuable to know. If, using more reporters, this LOV2 optogenetic technique shows the receptor only senses occupancy, that knowledge is incredibly valuable and would be a significant advance for the field.

Our data support an occupancy model of signaling through the CAR. That is, Zap70 recruitment is proportional to the number of bound CARs, and not sensitive to the ligand dwell time. This conclusion runs counter to the more widely held model of kinetic proofreading. What might account for the discrepancy? Of course, we have already noted that my experiments have only looked at Zap70 recruitment. But if the discrepancy persists even after looking at more distal signaling steps, is it possible that the CAR could use an occupancy model and the TCR still use kinetic proofreading? To the extent that CARs and the TCR use different mechanisms transmit extracellular ligand binding into intracellular ITAM phosphorylation, the greater the chance that CARs could be sensitive to occupancy while the TCR could be sensitive to binding kinetics. Therefore we need to consider several important differences between a CAR and the TCR, as well as technical limitation of my approach, which might explain why my results run counter to the more established kinetic proofreading model.

CARs are a single polypeptide with an extracellular binding domain and an intracellular ITAM signaling domain. By contrast, the native TCR complex is composed of eight polypeptide chains and coordinates with the CD4 or CD8 co-receptors, allowing for more subtle or complex mechanisms of receptor triggering. These more complex mechanism may be necessary for any putative kinetic proofreading by the TCR and would not be observed in experiments using a CAR. Below, I consider some important differences between a CAR and the TCR.

A major difference between a CAR and a TCR is their affinity for ligand. CARs typically have (and need) much higher affinity for their ligand than does the TCR. CARs respond best to ligands with a (3D)  $K_d$  of less than 300 nM<sup>13</sup>. By contrast pMHCs typically have a (3D)  $K_d$  of 1-10  $\mu$ M. It is possible that ITAM based receptors exhibit kinetic proofreading with low affinity, short binding ligands but use receptor occupancy for higher affinity ligands. This could happen if the receptors could only sense ligand dwell times below a certain threshold. Increasing ligand binding half-life past this threshold would not increase the specific activity of the receptor (as predicted by kinetic proofreading) but would simply increase the number of bound receptors.

In this light, the technical limitation of the optogenetic approach are important. Formally, we do not know the dwell time of LOV2 on an SLB for the Zdk-CAR as a function of blue light intensity. Measuring this “2D” dwell time is challenging and existing assays for TCR-pMHC dwell times can differ by an order of magnitude<sup>14-16</sup>. Attempting to rigorously repeat these assays for the LOV2:Zdk-CAR interaction was beyond the resources of this one graduate student. However, using a single molecule diffusion assay<sup>14</sup>, I was able to determine that LOV2 dissociates from the Zdk-CAR on the order of seconds with saturating blue light. By contrast, purified Zdk in solution dissociates from LOV2 on an SLB with a half-life of 700ms with saturating blue light (Fig. 7, Chapter 3). Thus it seems that LOV2-Zdk dissociation is slowed down slightly when confined to a “2D” environment.

If the fastest LOV2 ligand half-life was really on the order of seconds, it would (depending on which assay you believe) be an order of magnitude slower than a pMHC ligand. If ITAM-based receptors could only sense ligand binding half-lives of around a second or less, than it is possible that our optogenetic approach was not fast enough to catch this discrimination. (Though formally, kinetic proofreading does not put an upper limit on the ligand lifetimes the TCR could detect.) Once beyond the lifetime discrimination of the receptor, further decreases in ligand binding half-life would only result in greater receptor occupancy and



proportionally more signaling. Using point mutations in Zdk to weaken its interaction with LOV2 would be an effective way to decrease ligand binding half-lives to a regime similar to pMHC kinetics.

A CAR simplifies the TCR to an extracellular binding domain and an intracellular signaling domain. However, binding to the extracellular domain of the TCR is not always sufficient to cause signaling. For instance, the antibodies 2C11 and 17A2 both bind CD3 $\epsilon$  but only 2C11 is stimulatory<sup>12</sup>. This observations suggests that some specific, discriminatory mechanism exists to transmit extracellular ligand binding into intracellular signaling.

Although crystal structures of TCR  $\alpha\beta$  heterodimers unbound or bound to cognate pMHC have not shown any consistent changes to the tertiary structure, there is evidence that changes in the quaternary structure help promote signaling. Mammalian TCR  $\beta$  chains have a unique “FG loop” inserted into the constant domain that is proposed to interact with the CD3 $\epsilon\gamma$  dimer to promote signal transduction<sup>17</sup>. In one mechanosensitive TCR model, the pMHC applies a torque on the TCR  $\alpha\beta$  chains, causing them to rotate onto and reposition the neighboring CD3 $\epsilon\gamma$  dimer<sup>12</sup>. How this displacement promotes signaling is unclear, but could possibly promote the dissociation of the CD3 $\epsilon$  ITAM from the plasma membrane inner leaflet. Whatever the mechanism, this TCR specific “FG loop” is important for signaling. Deleting it reduces TCR sensitivity to pMHC by 1,000-10,000 fold, despite equal surface expression<sup>15</sup>. The FG loop could help the TCR transmit extra information about the ligand interaction (e.g. the amount of applied torque), aiding discrimination in a way a single chain CAR could not.

Another potential difference between the TCR and a CAR is the ability to protect ITAMs from phosphorylation by burying tyrosines in the inner leaflet of the plasma membrane. FRET data shows that the ITAM of CD3 $\epsilon$  is extended along the plasma membrane inner leaflet, as opposed to protruding into the cytoplasm in resting T cells<sup>10</sup>. NMR data shows the tyrosine of the ITAMs bury themselves in the inner leaflet, rendering them inaccessible to phosphorylation by Lck<sup>10</sup>. This association is mediated by the

interaction between negatively charged lipid head groups and an N-terminal positive patch on CD3 $\epsilon$ . Changing the local lipid composition or screening the charge-charge interaction by increased intracellular Ca<sup>2+</sup><sup>8</sup> have been suggested to release the CD3 $\epsilon$  ITAM from the membrane. However, there no direct evidence that CD3 $\zeta$  ITAMs are similarly protected and *in vitro* kinase assays show that it is weakly phosphorylated by Lck in the presence of lipid membranes.

These data could mean that CD3 $\epsilon$  ITAM release from the plasma membrane acts as a safety step prior to its phosphorylation and the recruitment of Zap70. The safety step could be one important step in kinetic proofreading that the CAR would not have, as mine and most all other CARs exclusively use the CD3 $\zeta$  ITAMS. Alternatively, even if the CD3 $\zeta$  ITAMs are protected in the inner leaflet, the CAR may not effectively change the local lipid environment and effectively not have this safety step. As a consequence, it could take a much higher affinity ligand to activate the CAR (as is generally the case) and not display kinetic proofreading.

TCRs are more constrained than CARs in the orientation in which they bind their ligands. A pMHC that was evolved to have high affinity for a purified TCR  $\alpha\beta$  ectodomain shows a drastic reduction in its affinity for the same TCR expressed in cells. As a consequence, it also is a poor agonist relative to other pMHCs with similar “3D” affinities<sup>18</sup>. The reduction in apparent affinity when the pMHC was presented in a “2D” environment could be because of limiting geometries with which the TCR and pMHC can interact. These constraints may reflect the need for co-receptor binding or some higher order association of TCRs to form<sup>18</sup>. By contrast, ligand orientation is not known to affect CAR signaling. (The distance the binding epitope is from the plasma membrane has been shown to affect CAR signaling, but not the orientation of the interaction per se.) The limited binding geometry that the TCR uses to recognize the pMHC could again point to a discrimination mechanism unique to the TCR and not used by a CAR.

There is increasing evidence that the TCR is mechanosensitive. Tangential (but not normal) pulling forces can make an otherwise non-stimulatory antibody stimulatory<sup>12,19,20</sup>. For one peptide series, it was shown that agonists form catch bonds with the TCR while non-agonists form slip bonds<sup>7</sup>. Catch bonds are interactions that increase their affinity under tension. (Imagine two hooks being pulled apart.) Slip bonds are the “usual” bonds that weaken under tension. This differential ability to form catch bonds would amplify affinity differences between agonist and non-agonist for the TCR while under tension. The pMHC-TCR interaction could be specialized to form the more uncommon catch bond, helping agonists to apply more force to the TCR and aid its activation. By contrast, CAR ligands almost certainly form slip bonds. Even if the CAR were mechanosensitive, it would be hard for non-pMHC ligands to apply the proper tangential force, owing to their slip bonds. Interestingly, T cells that are forced to recognize non-pMHC ligands (in mice lacking MHC I, MHC II, CD4 or CD8) have much higher ligand affinities; around 200nM<sup>21</sup>, which is just on the low end of what can stimulate a CAR<sup>13</sup>. In short, TCRs and CARs may differ in the ability to use mechanical cues to discriminate ligands.

In summary, one must be careful in using CARs to understand signaling properties of the native TCR. There are many potential mechanistic differences between how a TCR and a CAR recognize their ligands, as highlighted above. The more different the mechanisms, the more possible it is that the TCR could exhibit kinetic proofreading while the CAR could respond only to receptor occupancy. These caveats could be avoided by controlling pMHC association with a supported bilayer using the LOV2-Zdk interaction or (to a lesser extent) fusing Zdk directly to the TCR  $\alpha$  or  $\beta$  chain. Clearly, this would be a ripe area for future investigation.

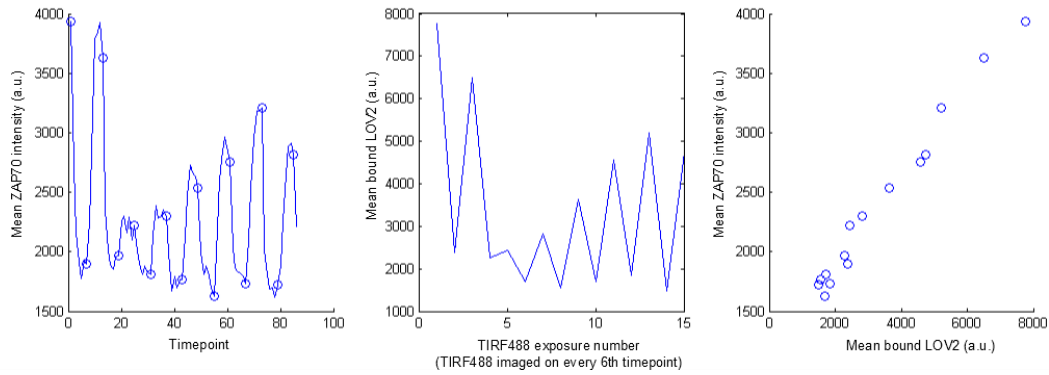


Figure 14: Example quantification of a light-stimulated time course

Clonal Jurkats expressing the Zdk-CAR (DT484), 10xHis CD148 (EX and TM domains; DT502) and the Zap70-mCherry reporter (DT523) were added to SLBs functionalized with LOV2-V529N (DT552) via a biotin-streptavidin linker. Cells were alternatively exposed to high and low intensity blue light, holding each intensity for 3 minutes (6 time points). (Left) Mean Zap70-mCherry intensity at the plasma membrane, as measured by TIRF561. The total Zap70-mCherry signal was divided by the area of cell footprint as determined by RICM. Open circles indicate the steady state value measured at the end of a 3 minute blue light exposure. (Middle) Mean bound LOV2 was measured less frequently, only at the end of a 3 minute blue light exposure, as the 488nm light used to image the conjugated Alexa-488 dye activates LOV2. Total LOV2 (after a flat field correction and background subtraction) was divided by cell area to produce the mean bound LOV2. (Right) Open circles represent the corresponding bound LOV2 (i.e. - receptor occupancy) and recruited Zap70-mCherry at the end of a 3 minute blue light exposure. Note that the points form a straight line, even though they were acquired non-sequentially. This strongly suggests the Zap70 recruitment is history independent.

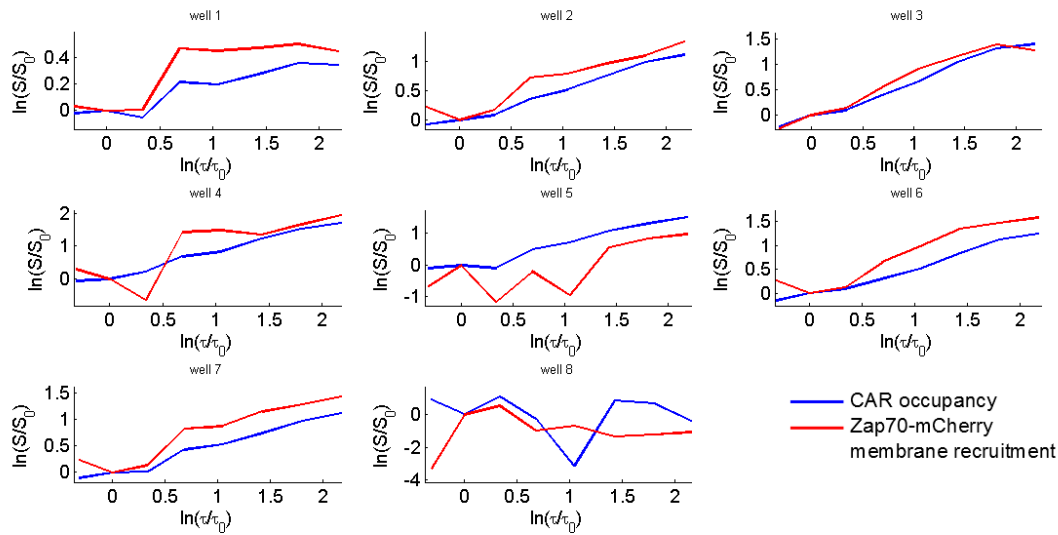


Figure 15: Zap70 recruits to the CAR without any proofreading steps

Log-log plots of either CAR occupancy or Zap70-mCherry membrane recruitment. Each well was functionalized with the following concentrations of LOV2-V529N (DT552): well 1 – 363 ng/ml, well 2 – 181 ng/ml, well 3 – 91 ng/ml, well 4 – 45 ng/ml, well 5 – 23 ng/ml, well 6 – 121 ng/ml, well 7 – 242 ng/ml, well 8 – 0 ng/ml.  $S$ : magnitude of signaling readout,  $\tau$ : LOV2-V592N binding half-life (as calculated from the reference curve in Figure 7, Chapter 1). In most wells with LOV2, the slope of CAR occupancy function is one or less, consistent with a one-step binding process. Significantly, the graph of Zap70-mCherry closely tracks the graph of CAR occupancy, indicating there are no proofreading steps prior to Zap70 recruitment. Zap70 recruitment is simply a reflection of CAR occupancy.

## References

1. McKeithan, T. W. Kinetic proofreading in T-cell receptor signal transduction. *Proc. Natl. Acad. Sci. U. S. A.* **92**, 5042–6 (1995).
2. Wu, J., Zhao, Q., Kurosaki, T. & Weiss, A. The Vav Binding Site (Y315) in ZAP-70 Is Critical for Antigen Receptor–mediated Signal Transduction. *J. Exp. Med.* **185**, (1997).
3. Magnan, A. *et al.* T Cell Development and T Cell Responses in Mice with Mutations Affecting Tyrosines 292 or 315 of the Zap-70 Protein Tyrosine Kinase. *J. Exp. Med.* **194**, (2001).
4. Di Bartolo, V. *et al.* Tyrosine 319, a newly identified phosphorylation site of ZAP-70, plays a critical role in T cell antigen receptor signaling. *J. Biol. Chem.* **274**, 6285–94 (1999).
5. Gong, Q. *et al.* Requirement for Tyrosine Residues 315 and 319 within  $\zeta$  Chain–Associated Protein 70 for T Cell Development. *J. Exp. Med.* **194**, (2001).
6. Yan, Q. *et al.* Structural basis for activation of ZAP-70 by phosphorylation of the SH2-kinase linker. *Mol. Cell. Biol.* **33**, 2188–201 (2013).
7. Liu, B., Chen, W., Evavold, B. D. & Zhu, C. Accumulation of dynamic catch bonds between TCR and agonist peptide–MHC triggers T cell signaling. *Cell* **157**, 357–368 (2014).
8. Shi, X. *et al.* Ca<sup>2+</sup> regulates T-cell receptor activation by modulating the charge property of lipids. *Nature* **493**, 111–115 (2012).
9. Gagnon, E., Schubert, D. A., Gordo, S., Chu, H. H. & Wucherpfennig, K. W. Local changes in lipid environment of TCR microclusters regulate membrane binding by the CD3 $\epsilon$  cytoplasmic domain. *J. Exp. Med.* **209**, (2012).
10. Xu, C. *et al.* Regulation of T Cell Receptor Activation by Dynamic Membrane Binding of the CD3 $\epsilon$

- Cytoplasmic Tyrosine-Based Motif. *Cell* **135**, 702–713 (2008).
11. Hu, K. H. & Butte, M. J. T cell activation requires force generation. *J. Cell Biol.* **213**, 535–542 (2016).
  12. Kim, S., Takeuchi, K., Sun, Z. & Touma, M. The  $\alpha\beta$  T cell receptor is an anisotropic mechanosensor. *J. Biol.* (2009).
  13. Chmielewski, M., Hombach, A., Heuser, C., Adams, G. P. & Abken, H. T Cell Activation by Antibody-Like Immunoreceptors: Increase in Affinity of the Single-Chain Fragment Domain above Threshold Does Not Increase T Cell Activation against Antigen-Positive Target Cells but Decreases Selectivity. *J. Immunol.* **173**, 7647–7653 (2004).
  14. O’Donoghue, G. P., Pielak, R. M., Smoligovets, A. a, Lin, J. J. & Groves, J. T. Direct single molecule measurement of TCR triggering by agonist pMHC in living primary T cells. *Elife* **2**, e00778 (2013).
  15. Axmann, M., Huppa, J. B., Davis, M. M. & Schütz, G. J. Determination of interaction kinetics between the T cell receptor and peptide-loaded MHC class II via single-molecule diffusion measurements. *Biophys. J.* **103**, 17–19 (2012).
  16. Huppa, J. B. *et al.* TCR-peptide-MHC interactions in situ show accelerated kinetics and increased affinity. *Nature* **463**, 963–7 (2010).
  17. Kim, S. T. *et al.* Distinctive CD3 Heterodimeric Ectodomain Topologies Maximize Antigen-Triggered Activation of T Cell Receptors. *J. Immunol.* **185**, 2951–2959 (2010).
  18. Adams, J. J. *et al.* T cell receptor signaling is limited by docking geometry to peptide-major histocompatibility complex. *Immunity* **35**, 681–93 (2011).
  19. Feng, Y. *et al.* Mechanosensing drives acuity of  $\alpha\beta$  T-cell recognition. *Proc. Natl. Acad. Sci.* 201703559 (2017). doi:10.1073/pnas.1703559114

20. Das, D. K. *et al.* Force-dependent transition in the T-cell receptor  $\beta$ -subunit allosterically regulates peptide discrimination and pMHC bond lifetime. *Proc. Natl. Acad. Sci.* **112**, 1517–1522 (2015).
21. Bunnell, S. C. *et al.* Persistence of cooperatively stabilized signaling clusters drives T-cell activation. *Mol. Cell. Biol.* **26**, 7155–66 (2006).



## CHAPTER FIVE: PROTOCOLS

### Protocol 1: PhyB purification

This purification starts with BL21(DE3) cells triply transformed with appropriate PhyB construct (e.g. DT266 or DT244) and two helper plasmids (DT243 and DT182) for synthesizing phytochromobilin in situ. Doing this transformation in one step requires commercially competent BL21(DE3) cells. I use the BL21(DE3) “Gold” cells from Agilent, though I don’t think the particular source matters. All media contains kanamycin (30 ug/ml), spectinomycin (50 ug/ml) and chloramphenicol (35 ug/ml). Personal notes about the protocol are in italics.

#### Day 1

- 1) Inoculate 1L of LB from a glycerol stock. Shake overnight at 37C in a 2.8L flask.

*I use a glycerol stock rather than doing a fresh transformation. As far as I can tell, I haven’t had problems because of it. If you shake at 30C, the culture sometimes isn’t turbid enough the next day. I’ve also grown the starter culture overnight at 30C and if they aren’t turbid enough the next day, shift them to 37C.*

#### Day 2

- 2) Back dilute the overnight LB culture 1:10 into TB. Grow at 37C to OD600 0.8. Shift to 18C for 30 minutes. Induce expression with 250uM IPTG. Shake overnight at 18C. Cover incubator with tin foil to block out light.

*I doubt the tin foil necessary, but I do it anyway. Superstition is that the free chromophore is light sensitive, but the PhyB-bound chromophore is more stable. During the actual purification, I don't go out of my way to protect it from ambient light.*

Days 3-4

- 3) Pellet cells at 4C.
- 4) Resuspend in IMAC binding buffer. 2ml buffer per 1g wet cell pellet. Add 1 Roche cOmplete™, Mini, EDTA-free tablet per 50ml of buffer.

*I'm skeptical the Roche tablets actually prevent any PhyB degradation. I forgot them once and didn't notice a significant change in the PhyB proteolysis products that co-purify. I think most of the PhyB proteolysis occurs in the cells prior to lysis. I tried the "InVision HisTag stain" to track proteolysis prior to cell lysis, but the expression was too low to track.*

- 5) Homogenize with dounce homogenizer.
- 6) Bring cells to 1mM PMSF and immediately lyse cells on Emulsiflex. I run the cells through twice so the lysate isn't gooey.
- 7) Hard spin. 40k RPM with a Ti45 rotor. (This is 185k RCF.)
- 8) Save and decant supernatant.
- 9) Recirculate supernatant over HiTrap Chelating column charged with Co<sup>2+</sup>, washed and equilibrated in IMAC binding buffer. Allow supernatant to pass over column at least once.

*I usually use the 1ml HiTrap Chelating column, as it's best scaled to the expected protein yield (1-2mg per 6L of culture). However, it can take a long time for all of the lysate to flow over the column. With a 6L prep, there is typically around 300ml of supernatant and the flow rate is around 1ml/min. I have let the rebinding go overnight with no ill effects. I have also successfully used the 5ml HiTrap Chelating columns, which allow the recirculation to go much faster.*

- 10) Wash column with IMAC binding buffer until effluent reads 60mAu (A280) or less.
- 11) Elute protein with a 10CV gradient elution. Buffer A: IMAC binding buffer. Buffer B: IMAC elution buffer.
- 12) Pool PhyB containing fractions. Concentrate to appropriate volume in anticipation of gel filtration.
- 13) Run concentrated PhyB over Superdex 200 Increase 10/300 GL column equilibrate with HBS.
- 14) Pool fractions and concentrate to approximately 1mg/ml.
- 15) Bring to 20% glycerol and snap freeze in liquid nitrogen. (I typically do 5ul aliquots.)

Qualitatively, I think roughly 50% of the PhyB molecules are active from this prep because when I do the Pif affinity prep, roughly half of the full length protein never binds to the Pif column.

## Protocol 2: Alternative PhyB purification with a Pif affinity column

Begins after step 11 of above protocol. This protocol ensures that 100% of PhyB molecules are active. It also eliminates the small amount of proteolytic fragments of PhyB that otherwise co-purify.

12) Pool PhyB fractions from IMAC elution.

13) Use HiPrep 26/10 Desalting column to exchange PhyB into HBS. Concentrate PhyB to approximately 5ml. Equilibrate Pif-functionalized GST column with HBS.

14) Slowly (0.2ml/min) run PhyB over the Pif column while illuminating it with red (650nm) light. Save PhyB containing effluent.

15) Extensively wash the Pif column at 1ml/min with HBS until effluent has an A280 of 10mAu or less.

16) Under a slow flow rate (0.2 ml/min), turn off the red light and turn on the infra-red (750 nm) light. Immediately start collecting the effluent. The peak is typically ~4ml with a peak of ~50-100mAu.

17) Repeat steps 14-16 1-3 more times until PhyB eluted from the Pif columns drops significantly.

18) Pool PhyB contain elution fractions. Concentrate to appropriate volume in anticipation of gel filtration.

19) Run concentrated PhyB over Superdex 200 Increase 10/300 GL column equilibrate with HBS.

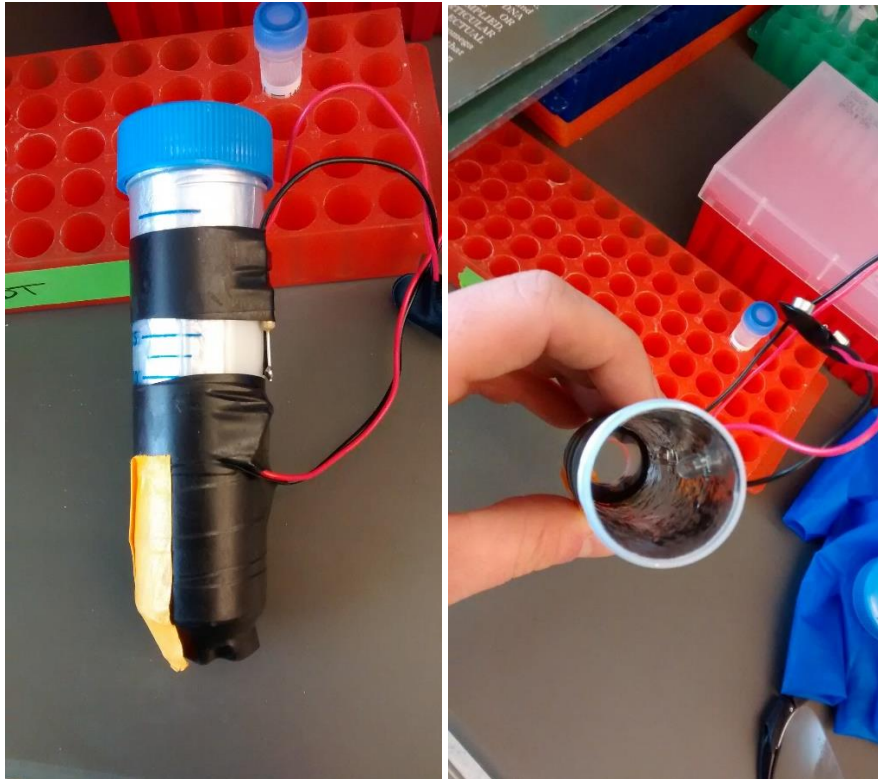
20) Pool fractions and concentrate to approximately 1mg/ml.

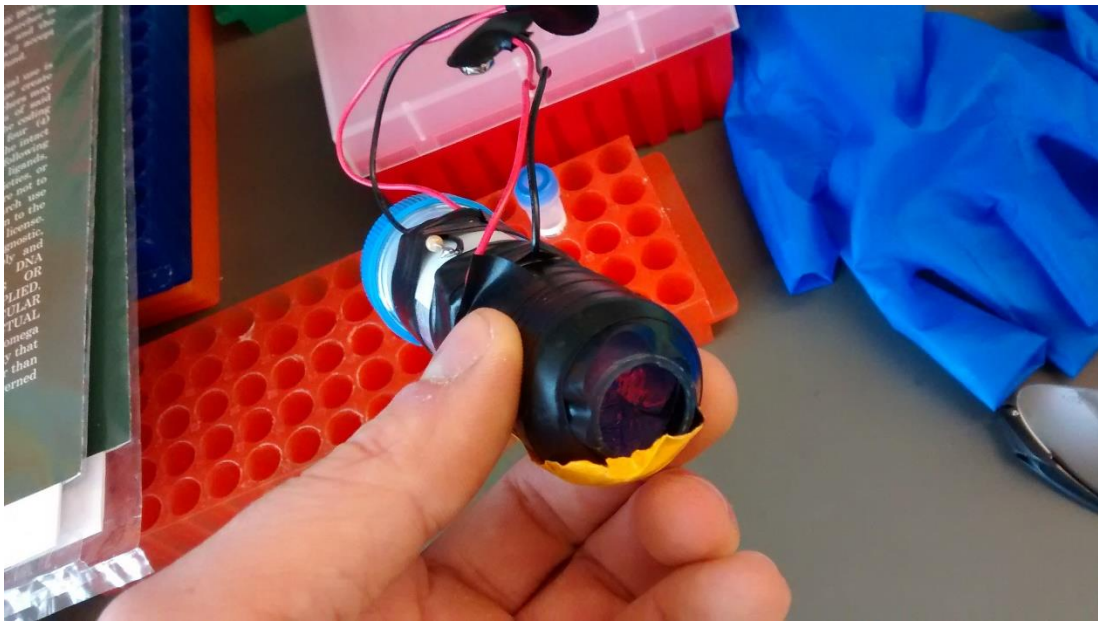
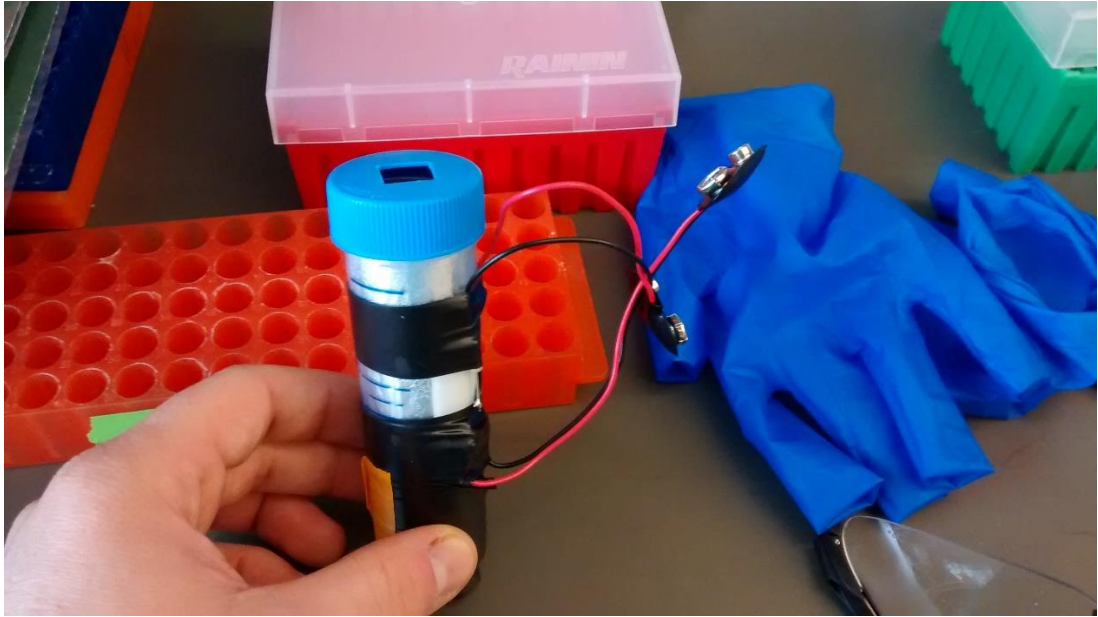
21) Bring to 10% glycerol and snap freeze in liquid nitrogen. (I typically do 5ul aliquots.)

### Light box for binding and eluting PhyB with light

For binding and eluting PhyB with light, I made a custom "light box" out of a 50ml Falcon tube. I used some spray adhesive to line the inside of the tube with tin foil, shiny side pointing inside. I inserted one

red and one infra-red LED through small holes cut in the side. The bottom and part of the top were cut so that a 1ml column and tubing can fit inside. All exposed holes are covered with lab tape when binding and eluting with light. LEDs are soldered in series with a 1 kOhm resistor and run with a 9V battery. Pictures below:





## Protocol 3: Pif conjugated protein purification

This is the general protocol I use for purifying most all of my Pif tagged proteins.

### Day 1

- 1) Inoculate LB with appropriate strain. Shake overnight at 30C.

### Day 2

- 2) Back dilute the overnight LB culture 1:10 into TB. Grow at 37C to OD600 0.8. Shift to 18C for 30 minutes. Induce expression with 250uM IPTG. Shake overnight at 18C.
- 3) Pellet cell at 4C.
- 4) Resuspend in IMAC binding buffer. 2ml buffer per 1g wet cell pellet.
- 5) Homogenize with dounce homogenizer.
- 6) Bring cells to 1mM PMSF and immediately lyse cells on Emulsiflex. I run the cells through twice so the lysate isn't gooey.
- 7) Hard spin. 40k RPM with a Ti45 rotor. (This is 185k RCF.)
- 8) Save and decant supernatant.
- 9) Recirculate supernatant over a 5ml HiTrap chelating column charged with  $\text{Co}^{2+}$ , washed and equilibrated in IMAC binding buffer. Allow supernatant to pass over column at least once.
- 10) Wash column with IMAC binding buffer until effluent reads 60mAu (A280) or less.
- 11) Elute protein with a 10CV gradient elution. Buffer A: IMAC binding buffer. Buffer B: IMAC elution buffer.
- 12) Pool protein containing fractions and desalt back into IMAC binding buffer using a HiPrep 26/10 Desalting column.
- 13) Add SenP2-6xHis (1:1000 w/w) and digest overnight at 4C.

### Day 3

- 14) Recirculate protein over the used HiTrap Chelating column, equilibrated in IMAC binding buffer.
- 15) Concentrate flow through and run over appropriate gel filtration column, equilibrated in HBS.
- 16) Pool fractions and concentrate to at least 1mg/ml. Bring to 10% glycerol and snap freeze aliquots in liquid nitrogen.



## Protocol 4: LOV2 purification

Used for purifying DT493 or similar proteins.

### Day 1

1. Inoculate 200ml of LB +Kan +Cam with E. coli BL21(DE3) doubly transformed with the appropriate LOV2 plasmid and the BirA expressing helper plasmid (DT311). Incubate shaking overnight at 30C.

### Day 2

2. Dilute the overnight LB culture 1:10 into 1L of TB media +Kan +Cam in a 2.8L baffled flask. Shake at 180 rpm at 37C. Cover any exposed windows of the shaker with tinfoil.
3. When the cultures reach an OD600 of 0.6-0.8, reduce the temperature to 18C. After 30 minutes, induce expression by adding IPTG to a final concentration of 250nM. Biotin is added to a final concentration of 50uM. The biotin stock solution is 5mM biotin in 10mM Tris-HCL, pH 8.3. Extra flavin mononucleotide (FMN) is added to a final concentration of (??? CHECK THIS), from a ????? stock solution.
4. Shake cultures at 180 rpm and 18C overnight.

### Day 3

5. Pellet cells at 4C.
6. Resuspend in IMAC binding buffer. 2ml buffer per 1g wet cell pellet. Add 1 Roche cOmplete™, Mini, EDTA-free tablet per 50ml of buffer.
7. Homogenize with dounce homogenizer.
8. Bring cells to 1mM PMSF and immediately lyse cells with an Emulsiflex. I run the cells through twice so the lysate isn't gooey.

9. Hard spin. 40k RPM with a Ti45 rotor. (This is 185k RCF.)
10. Save and decant supernatant.
11. Recirculate supernatant over HiTrap Chelating column charged with  $\text{Co}^{2+}$ , washed and equilibrated in IMAC binding buffer. Allow supernatant to pass over column at least once.
12. Wash column with IMAC binding buffer until effluent reads 60mAu (A280) or less.
13. Elute protein with a 10CV gradient elution. Buffer A: IMAC binding buffer. Buffer B: IMAC elution buffer.
14. Pool LOV2 containing fractions (they should be light yellow) and exchange into IMAC binding buffer using a desalting column.
15. Add 6xHis-TEV protease at a ratio of 1:10 w/w, TEV:LOV2. Incubate overnight at 4C, wrapped in tinfoil.

#### Day4

16. Run the overnight cleavage mixture over a HiTrap Chelating column, freshly charged with  $\text{Co}^{2+}$  several times.
17. Take the HiTrap flow through and exchange into HBS + 0.5mM TCEP with a desalting column.
18. Concentrate the protein to around 3-4 mg/ml. It doesn't have to be exact, but you don't want it to be dilute for dye labeling.
19. Add the appropriate maleimide dye at a ratio of molar ratio of 1:2, protein to dye. (10mM stock solution in DMSO.) Quickly mix and incubate on ice for 30 seconds. Quench the reaction by bringing it to a final DTT concentration of 10mM.

This fast labeling at a low molar ratio is done to bias maleimide reaction with the KCK tag cysteine, rather than the LOV2 active site cysteine. A time course of dye labeling showed the reaction reaches a plateau by 30 seconds and shows no further increase up to two hours later. Considering

this protocol labels over 50% of the LOV2 molecules and that LOV2 shows no obvious decline in activity after labeling, I believe this protocol does not cause significant modification of the active site cysteine in LOV2.

20. Run the dye-labeled LOV2 over a Superdex 200 Increase 10/300 GL column equilibrate with HBS.
21. Concentrate protein to greater than 1 mg/ml. Bring the protein solution to 10% glycerol. Aliquot (typically 3ul) and snap freeze in liquid nitrogen. Store at -80C.

## Protocol 5: Zdk purification

I used a procedure identical to the LOV2 purification to purify dye-labeled SpyCatcher-Zdk (DT482) with the following common sense modifications.

1. Growth media only contains Kan. There is no extra biotin or flavin mononucleotide. Bacteria are not co-transformed with the BirA expression plasmid.
2. The SUMO protease 6xHis-SenP2 is added to the IMAC eluted protein at 1:1000 w/w instead of TEV protease.
3. Higher ratios of dye and longer incubation periods can be used to label the protein, as there is only one unique cysteine that can be labeled.

## Protocol 6: Buffer recipes for protein purification

### IMAC binding buffer

50mM  $\text{KH}_2\text{PO}_4$

400mM NaCl

0.5mM BME

Adjust to pH 7.5

### IMAC elution buffer

50mM  $\text{KH}_2\text{PO}_4$

400mM NaCl

500mM imidazole

0.5mM BME

Adjust to pH 7.5

### HBS

20mM HEPES

100mM KCl

0.5mM TCEP

Adjust to pH 7.5

PBS

15mM NaH<sub>2</sub>PO<sub>4</sub>

150mM NaCl

0.5mM BME

Adjust to pH 7.4

Terrific Broth (TB) – 1 liter

*Nutrient Base*

12g tryptone

24g yeast extract

4ml glycerol

900ml ddH<sub>2</sub>O

*10x TB Salts*

170mM KH<sub>2</sub>PO<sub>4</sub>

720mM K<sub>2</sub>HPO<sub>4</sub>

Autoclave the nutrient base and 10x TB salts separately. Then add 100ml of 10x TB salts to 900ml of the nutrient base to make 1L of TB.

## Protocol 7: SUV formation

### Lipid mix

SUVs can be made from many different lipids and with different molar ratios. I make separate batches of SUVs with the following ratios.

Lipid	Molar Ratio	Lipid	Molar Ratio
POPC	97.5	POPC	97.5
PEG-PE	0.5	PEG-PE	0.5
DGS-NTA(Ni)	2	Biotinyl Cap PE	2

The ordering information from Avanti is:

Lipid	Avanti #
POPC	850457C
PEG-PE	880230C
DGS-NTA(Ni)	790404C
Biotinyl Cap PE	870277X



Note that the biotinyl Cap PE lipids (870277X) come pre-dissolved in a solution of CHCl<sub>3</sub>/MeOH/H<sub>2</sub>O. They will turn cloudy when added to the other lipids that are dissolved only in chloroform. It's nothing to worry about. Dry them down and precede with the protocol.

#### Clean all glassware that will contact the lipids

1. Place 6-8 glass vials and ~10 glass pasture pipettes in a 1L beaker
2. Cover with 3M NaOH. Sonicate for 20-30 minutes. Save the strong base for cleaning other glass. It can be used multiple times.
3. Wash glass vials 5-6x with milliQ. I handle the glass with Nitrile powder-free gloves. You don't want fluorescent crap from your gloves getting into the mix.
4. Add 5% Hellmanex solution that has been heated in the microwave for 1 minute. Gently swirl. Vials can be left in the hellmanex for a long time – over night.
5. Decant Hellmanex and wash glass vials 10X with milliQ. I normally do this at the milliQ. You really want to remove all the hellmanex. This will play total havoc with your lipids, especially if you are storing your stock lipids in these vials.
6. While cleaning vials, take caps and sonicate in ddH<sub>2</sub>O with several washes. Oven dry caps with glass vials.
7. Oven dry at 80C to remove water.
8. Cap the vials and keep away from dust. Vial cleaned this way are generally good for a month.

#### Dry down lipids and rehydrate

1. Take clean glass vials and rinse 2x with EM grade chloroform. Rinse vigorously – this way you remove any traces of hellmanex or organic contaminates.

2. In a 4mL clean glass vial (see protocol above), add ~500µl of EM grade chloroform using a cleaned pasture pipettes.
3. Add lipids (**4 µmoles total**) in desired ratio to glass vials. Use Hamilton syringe that is chloroform resistant. If using Rhodamine-PE, just add a trace amount by dipping the tip of a cleaned pasture pipette into the Rhodamine-PE stock, then into your lipid mixture.
4. Dry down lipids by flowing nitrogen gas over vial opening. Slowly rotate with your hands until the chloroform evaporates, about 5 minutes.
5. Vacuum dry in desiccator for 2 hours or overnight. I usually dry down overnight.
6. Rehydrate with 1.5mL of 0.22µm filtered dPBS. (I use dPBS with Ca<sup>2+</sup> and Mg<sup>2+</sup>, but don't think it matters.)
7. Re-suspend for 10min by vortexing at moderate speed. Don't go too fast or you will make bubbles. Transfer to 1.5 mL epi. Fill epi with nitrogen and close while flowing nitrogen over the epi.
8. Freeze with liquid nitrogen.

#### Freeze/thaw method for making SUVs

1. Thaw 1.5ml of lipid rehydrated lipids, in cold water bath. Slow thawing helps to break up the multilamellar vesicles.
2. Plunge into liquid nitrogen, thaw in 42C heating block with water, repeat. Perform freeze thaw cycle 20 times. You will see the lipid suspension turn clear, this is an indication that multilamellar vesicles have been broken down.
3. Centrifuge at max speed on a table top centrifuge at 4C for 30 minutes. Note this is an important step and creates a more homogenous SUV suspension.
4. Remove top 80% of supernatant and transfer to a new tube.

5. Make 30ul aliquots. Close under nitrogen flow. Store in liquid nitrogen until ready to use. I find the SUVs are good in liquid nitrogen for 6 months. Although SUVs can last several days at 4C, I generally don't store them once thawed from liquid nitrogen storage.

## Protocol 8: RCA glass coverslip cleaning

1. Add 5 25x75mm glass coverslips (Ibidi catalogue #10812) to an upright glass coverslip holder.
2. Cover with acetone. Bath sonicate for 10 minutes.
3. Discard acetone. Add 196 proof ethanol to cover. Bath sonicate for 10 minutes.
4. Discard ethanol. Rinse 5 times with ddH<sub>2</sub>O. Cover slides with ddH<sub>2</sub>O and bath sonicate 10 minutes.
5. Discard water and rinse several more times with ddH<sub>2</sub>O to remove any trace organic solvents.
6. Dissolve 3.75g KOH in 45ml of ~50C water and add to the slides. The hot water helps to reduce thermal expansion/contraction wear on the coverslip holder.
7. Add 15ml of 30% hydrogen peroxide. The mixture should cover the slides.
8. Place coverslip holder in a 70-80C water bath. Let react for 10 minutes. There should be moderate to strong bubble formation.
9. Remove coverslip holder from the water bath and carefully decant the solution.
10. Wash coverslips 5 times with ~50C ddH<sub>2</sub>O.
11. To the coverslips, add in order: 38ml ~50C ddH<sub>2</sub>O, 9.5ml 37% HCl and 12.6 ml 30% hydrogen peroxide.
12. Place holder in the 70-80C water bath and react for 10 minute. Bubble formation should be moderate, but less vigorous than during the base etch.
13. Remove the coverslip holder from the water bath and carefully decant the solution.
14. Wash coverslips 5 times with ~50C ddH<sub>2</sub>O.
15. Cover the coverslips with ddH<sub>2</sub>O and a lid until ready to use. Coverslips are good up to a week after cleaning.

## Protocol 9: Kinetic proofreading experiments

1. Remove an RCA cleaned glass coverslip and quickly blow dry with compressed nitrogen.
2. Secure a 6-channel Ibidi sticky chamber on top of an RCA cleaned glass coverslip. Press firmly and let stand for four minutes before further use. This helps the adhesive set, and prevents leaking and channel-to-channel cross contamination during use.
3. Dilute 30ul of SUVs into 800ul of 0.22um filtered dPBS. (I use +Ca/Mg, but it doesn't matter.) I usually use 15ul of Ni-NTA SUVs and 15ul of biotinyl Cap PE SUVs.
4. Add approximately 100ul of the diluted SUVs to each channel and incubate at 37C in a humidified tissue culture incubator for 1 hour.
5. Flush a channel with 500ul filtered dPBS to remove excess SUVs.
6. Add ~100ul streptavidin, diluted 1ug/ml in dPBS + 1mg/ml beta casein, 0.5mM BME, 0.22um filtered. Incubate at room temperature for 5 minutes.
7. Flush channel with 500ul filtered dPBS.
8. Add biotinylated LOV2 diluted into dPBS + 1mg/ml beta casein, 0.5mM BME, 0.22um filtered. Typical concentrations ranged from 100ng/ml to 10ng/ml. Typically LOV2 V529N (DT552) was used, as the destabilized mutant has better Zdk-CAR release kinetics than wt LOV2. Incubate at room temperature for 5 minutes.
9. Flush channel with 500ul filtered dPBS.
10. Flush channel with 200ul dPBS + 1mg/ml beta casein, 0.5mM BME, 50ug/ml ascorbic acid that has been pretreated with an oxygen scavenger (ProLong Live Antifade Reagent, ThermoFisher Scientific) for at least 90 minutes at room temp. REMOVING OXYGEN IS ABSOLUTELY REQUIRED, AS THE LOV2 WILL BLEACH AFTER ~10-15 MINUTES OF BLUE LIGHT LED EXPOSURE. PRETREATMENTS LESS THAN 90 MINUTES DO NOT FULLY REMOVE DISSOLVED OXYGEN.

11. Add cell that have been washed into dPBS + 1mg/ml beta casein, 0.5mM BME and then washed into dPBS + 1mg/ml beta casein, 0.5mM BME, 50ug/ml ascorbic acid that has been pretreated with an oxygen scavenger.
12. Let cells settle for ~5 minutes in the dark and then begin imaging.
13. Typically, images of TIRF561, RICM (reflection interference contrast microscopy, using 561±30nm band pass filter with a xenon arc lamp) and of projected blue light were taken every 30 seconds. Every 3 minutes, once cells had reached steady state for a given intensity blue light, images of TIRF561, RICM, projected blue light, TIRF488 were taken, *in that order*. Blue light from TIRF488 quickly affects Zap70-mCherry recruitment.

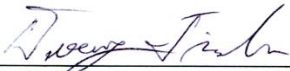
There were typically 10 blue light LED values held in one time course, each held for 3 minutes and evenly log spaced to cover minimal and maximal Zap70-mCherry recruitment. Log-even spacing insured (roughly) linearly spaced ligand binding half-lives.

**Publishing Agreement**

*It is the policy of the University to encourage the distribution of all theses, dissertations, and manuscripts. Copies of all UCSF theses, dissertations, and manuscripts will be routed to the library via the Graduate Division. The library will make all theses, dissertations, and manuscripts accessible to the public and will preserve these to the best of their abilities, in perpetuity.*

**Please sign the following statement:**

*I hereby grant permission to the Graduate Division of the University of California, San Francisco to release copies of my thesis, dissertation, or manuscript to the Campus Library to provide access and preservation, in whole or in part, in perpetuity.*

  
\_\_\_\_\_  
Author Signature

8/30/17  
Date